Separation and fractionation of nanoparticles in solutions by membranes

Asmaa Khaled Selim

Thesis submitted to the Faculty of Science at the University of Zaragoza, Spain in partial fulfilment of the requirements for the degree of

Master Erasmus Mundus

In
Membrane Engineering

Supervisors: Dr. Reyes Mallada
Dr. Pilar Lobera

June 24, 2014

Zaragoza, Spain

Disclaim

BG Този проект е финансиран с подкрепата на Европейската комисия. Тази публикация (съобщение) отразява само личните виждания на нейния автор и от Комисията не може да бъде търсена отговорност за използването на съдържащата се в нея информация.

CS Tento projekt byl realizován za finanční podpory Evropské unie. Za obsah publikací (sdělení) odpovídá výlučně autor. Publikace (sdělení) nereprezentují názory Evropské komise a Evropská komise neodpovídá za použití informací, jež jsou jejich obsahem.

DA Dette projekt er finansieret med støtte fra Europa-Kommissionen. Denne publikation (meddelelse) forpligter kun forfatteren, og Kommissionen kan ikke drages til ansvar for brug af oplysningerne heri.

DE Dieses Projekt wurde mit Unterstützung der Europäischen Kommission finanziert. Die Verantwortung für den Inhalt dieser Veröffentlichung (Mitteilung) trägt allein der Verfasser; die Kommission haftet nicht für die weitere Verwendung der darin enthaltenen Angaben.

ΕΛ Το σχέδιο αυτό χρηματοδοτήθηκε με την υποστήριξη της Ευρωπαϊκής Επιτροπής.Η παρούσα δημοσίευση (ανακοίνωση) δεσμεύει μόνο τον συντάκη της και η Επιτροπή δενευθύνεται για τυχόν χρήση των πληροφοριών που περιέχονται σε αυτήν.

EN This project has been funded with support from the European Commission. This publication (communication) reflects the views only of the author, and the Commission cannot be held responsible for any use which may be made of the information contained therein.

ES El presente proyecto ha sido financiado con el apoyo de la Comisión Europea. Esta publicación (comunicación) es responsabilidad exclusiva de su autor. La Comisión no es responsable del uso que pueda hacerse de la información aquí difundida.

ET Projekti on rahaliselt toetanud Euroopa Komisjon. Publikatsiooni sisu peegeldab autori seisukohti ja

Euroopa Komisjon ei ole vastutav selles sisalduva informatsiooni kasutamise eest.

FI Hanke on rahoitettu Euroopan komission tuella.Tästä julkaisusta (tiedotteesta) vastaa ainoastaan sen laatija, eikä komissio ole vastuussa siihen sisältyvien tietojen mahdollisesta käytöstä.

FR Ce projet a été financé avec le soutien de la Commission européenne. Cette publication (communication) n'engage que son auteur et la Commission n'est pas responsable de l'usage qui pourrait être fait des informations qui y sont contenues.

GA Maoiníodh an tionscadal seo le tacaíocht ón gCoimisiún Eorpach. Tuairimí an údair amháin atá san fhoilseachán (scéala) seo, agus ní bheidh an Coimisiún freagrach as aon úsáid a d'fhéadfaí a bhaint as an eolas atá ann.

HU Az Európai Bizottság támogatást nyújtott ennek a projektnek a költségeihez. Ez a kiadvány (közlemény) a szerzõ nézeteit tükrözi, és az Európai Bizottság nem tehetõ felelõssé az abban foglaltak bárminemû felhasználásért.

IT Il presente progetto è finanziato con il sostegno della Commissione europea. L'autore è il solo responsabile di questa pubblicazione (comunicazione) e la Commissione declina ogni responsabilità sull'uso che potrà essere fatto delle informazioni in essa contenute.

NL Dit project werd gefinancierd met de steun van de Europese Commissie. De verantwoordelijkheid voor deze publicatie (mededeling) ligt uitsluitend bij de auteur; de Commissie kan niet aansprakelijk worden gesteld voor het gebruik van de informatie die erin is vervat.

LT Šis projektas finansuojamas remiant Europos Komisijai. Šis leidinys (pranešimas) atspindi tik autoriaus požiūrį, todėl Komisija negali būti laikoma atsakinga už bet kokį jame pateikiamos informacijos naudojimą.

LV Šis projekts tika finansēts ar Eiropas Komisijas atbalstu. Šī publikācija (paziņojums) atspoguļo vienīgi autora uzskatus, un Komisijai nevar uzlikt atbildību par tajā ietvertās informācijas jebkuru iespējamo

izlietojumu.

MT Dan il-proġett ġie finanzjat bl-għajnuna tal-Kummissjoni Ewropea. Din il-publikazzjoni tirrifletti (Dan il-komunikat jirrifletti) l-opinjonijiet ta' l-awtur biss, u l-Kummissjoni ma tistax tinżamm responsabbli għal kull tip ta' uzu li jista' jsir mill-informazzjoni li tinsab fiha (fih).

PL Ten projekt został zrealizowany przy wsparciu finansowym Komisji Europejskiej. Projekt lub publikacja odzwierciedlają jedynie stanowisko ich autora i Komisja Europejska nie ponosi odpowiedzialności za umieszczoną w nich zawartość merytoryczną.

PT Projecto financiado com o apoio da Comissão Europeia. A informação contida nesta publicação (comunicação) vincula exclusivamente o autor, não sendo a Comissão responsável pela utilização que dela possa ser feita.

RO Acest proiect a fost finanţat cu sprijinul Comisiei Europene.<0}Această publicaţie (comunicare) reflectă numai punctul de vedere al autorului şi Comisia nu este responsabilă pentru eventuala utilizare a informaţiilor pe care le conţine.

SK Tento projekt bol financovaný s podporou Európskej Komisie. Táto publikácia (dokument) reprezentuje výlučne názor autora a Komisia nezodpovedá za akékoľvek použitie informácií obsiahnutých v tejto publikácii (dokumente).

SL Izvedba tega projekta je financirana s strani Evropske komisije. Vsebina publikacije (komunikacije) je izključno odgovornost avtorja in v nobenem primeru ne predstavlja stališč Evropske komisije.

SV Projektet genomförs med ekonomiskt stöd från Europeiska kommissionen. Föruppgifterna i denna publikation (som är ett meddelande) ansvarar endast upphovsmannen. Europeiska kommissionen tar inget ansvar för hur dessa uppgifter kan komma att användas

Acknowledgment

First of all, I express my utmost thanks to Almighty God the omnipresent and the creator of the worlds, who has endowed me brain and instable instinct, construction of knowledge and body to accomplishs work.

After this, I would like express my deepest gratitude to my advisor, Professor Reyes Mallada for her support and guidance through this experience. Whatever kind of problem was discussed, her advice and encouragement always provided new perspectives. The expertise that she shared with me remains a source for my professional carrier. I am very thankful for everything she has done, for me. I warmly thank Dr. Maria Pilar Lobera and Ana for their advice and participation as my committee members.

Also, I would like to voice my appreciation to Maciej Zieba and Dr. Nuria Navascues Garcia for giving technical suggestions, and providing me the use of many lab facilities, their time, encouragement, suggestions, and the sharing of their expertise and special thanks for Nuria for her help with transmission electron microscopy. I am also grateful to Carlos Ayllón for his help as well for scanning electron microscopy.

I would also like to thank my mother, my sister and the rest of my family and my fiancé, for their continued support over the two years of this master. I would also like to appreciate all my friends namely Usman, Vinit, Ghada, Meron and Cheryl for their supporting and motivation.

Table of contents

List of figures

List of tables

Resumen

Las interesantes propiedades dependientes de la forma y tamaño de las nanopartículas han conseguido llamar la atención recientemente en muchas áreas científicas y de ingeniería. Hoy en día, las nanopartículas tienen una amplia gama de aplicaciones en el campo de purificación de agua. Cuando se usan nanopartículas para eliminar contaminantes y purificar el agua, dichos contaminantes y nanopartículas deben eliminarse de la corriente purificada. Por esta razón es importante desarrollar un método de separación y purificación selectiva según el tamaño de la nanopartícula. Las técnicas de filtración tienen la ventaja de que son fáciles, rápidas y verdes.

Esta tesis presenta nuevos enfoques para el uso de membranas de ultrafiltración para la separación y purificación de las nanopartículas mediante técnicas de filtración sin salida y de flujo cruzado. Se ha evaluado una membrana cerámica comercial para el fraccionamiento y separación de nanopartículas se plata y sílice. Con el fin de estudiar los aspectos del proceso de filtración, se sintetizaron nanopartículas de plata y de sílice.

Las nanopartículas y la solución antes y después de la filtración se caracterizaron por microscopía electrónica de barrido (SEM), TEM para revelar su formación y correspondientes morfologías, dispersión de luz dinámica (DLS) para la distribución de la partícula en función de tamaño, Radwag para la concentración y finalmente una espectroscopía de luz ultravioleta visible (UV-vis) para detectar los distintos espectros de las nanopartículas de plata producidas.

Abstract

The intriguing size and shape dependent properties of nanoparticles have garnered recent attention in many science and engineering areas. Nowadays, nanoparticles have wide range of applications in the water purification field. When applying nanoparticles for removing contaminants / water purification, nanoparticles and the contaminant should be removed from the purified stream. For these reasons it is important to develop a method for size selective separation and purification of nanoparticles. Membrane filtration technique has been chosen for the separation and purification of water from those nanoparticles, because of their advantages of being easy, fast and green technique.

This thesis presents novel approaches of using ultrafiltration membranes for nanoparticle separation and purification, using dead-end and cross-flow filtration techniques. A commercial ceramic membrane was evaluated for the fractionation and separation of silver and silica nanoparticles. In order to study the filtration process aspects, silver nanoparticles and silica nanoparticles were synthesized.

Characterization of both nanoparticles and the solution before and after filtration was adopted using by Scanning Electron Microscopy (SEM), TEM to disclose their formation and corresponding morphologies, dynamic light scattering (DLS) particle size analyser for particle size distribution, RadWag for concentration and finally Ultraviolet visible (UV-vis) scanning spectrophotoscopy to detect the distinct spectrum of the silver nanoparticles produced.

Chapter one: Introduction

1.1 Background

Nanotechnology is the science and engineering of examining, monitoring, and modifying the behavior and performance of materials at nanoscale that is, at the atomic or molecular level. The techniques and principles have gained recognition in the field of medicine, water filtration and, in several industries and underdevelopment into transportation applications. Nanotechnology is multidisciplinary and has motivated collaboration among engineers, scientists, innovators, and researchers in sustainable development.[1]

Nanotechnology is an emerging field that covers a wide range of technologies, which are presently under development in nanoscale. It plays a major role in the development of innovative methods to produce new products, to substitute existing production equipment and to reformulate new materials and chemicals with improved performance resulting in less consumption of energy and materials and reduced harm to the environment as well as environmental remediation.

Similar to nanotechnology's success in consumer products and other sectors, nanoscale materials have the potential to improve the environment, both through direct applications of those materials to detect, prevent, and remove pollutants, as well as indirectly by using nanotechnology to design cleaner industrial processes and create environmentally responsible products [2].

In the area of water purification, nanotechnology offers the possibility of an efficient removal of pollutants and germs [3]. Nanoparticles have been used for remediation of the ground water and for many other applications.

It must be remembered that nanoparticles– unlike atoms– are never monodisperse and no two particles are identical. If the nanoparticles are monodisperse, they are a single-size and their properties are easily defined; however, if the nanoparticles are produced by attrition, they are polydisperse and their properties over a broad range when compared to single-size nanoparticles

[1]. This inherent polydispersity complexities of self-assembly, affects the overall characteristics deriving from the size-dependent properties of individual nanoparticles [4].

The impact of manufactured nanoparticles on living organisms is still controversial, albeit most researchers consider them as toxic. Engineered nanoparticles have the ability to travel from the lung to systematic sites in case of inhaling them. In addition, they have high rate of pulmonary deposition, penetrate dermal barriers and general high inflammatory potency. [5]

Therefore, the sustainable growth of nanotechnology requires an environmentally-friendly technology to remove nanoparticles from potential drinking water sources [6]. These nanoparticles are synthesised in liquid media and usually the concentration of nanoparticles in the final solution is very low. For these reasons is important to develop a method for size selective separation and purification of nanoparticles.

Nanoparticles size is one of the most important characterization parameter. In addition, size, morphology and structure are the effective factors on the nanoparticles performance. Producing controlled size and size distribution of nanoparticles was and still one of the confrontations, which stand up to nanoparticles production.

Long time ago, producing a monodisperesd nanoparticles had been achieved by either controlling the production process or through the fractionation and separations techniques of nanoparticles. [7]

The purification and separation of nanoparticles is also challenging because nanoparticles do not typically dissolve in solution, but instead disperse in the solvent: each individual nanoparticle exists as a single particle or crystal in the liquid system.

1.2 Separation and fractionation methods

Approaches to separation and purification of nanoparticles are based on methods routinely applied to inorganic and organic materials and macromolecules, and may be selective for material property or size.

Nanoparticles often consist of an inorganic (metal) core decorated with organic ligands. Purification and separation strategies for these molecules are capitalize on differences in their chemical and physical properties, such as polarity, solubility, and molecular weight, and due to the size differences of nanoparticles and their byproducts , it is possible to isolate them.

Techniques such as magnetic fields, chromatography, density gradient centrifugal, electrophoresis, selective precipitation, liquid- liquid extraction, and field-flow fractionation were usually used to separate and fractionate the nanoparticles.

Table 1, is showing a summary of those different technique in terms of the driving force, main advantages and disadvantages of each. In addition, table one is showing the most famous techniques which are used in nanoparticles separation specifically.

Table 1: Summary of separation and fractionation methods

Method	Driving force& Properties	Advantages	Disadvantages	Most famous technique	Ref.
Magnetic field	-Magnetic force - Based on the NPs magnetic susceptibility	- Doesn't need addition of surfactant - Fast technique	Limited by 50 nm	- Magnetic field flow fractionation - High gradient magnetic separation	[4]
Chromatography	- Based on differences in partition coefficient between mobile and stationary phases	-Working in a wide range of NPs (few tens to few hundred)	- Clogging the pores of the packing material	- High performance liquid chromatography - Size-exclusion chromatography	[1]
Centrifugal	- Based on density differences	-Simple and easy - cheap	- Time consuming - Limited amount of sample depending on the tube size - Required high speed for high efficiency	- Density gradient centrifugal and ultracentrifugal	[4], [1]
Electrophoresis	- Electric field - Based on the charge of the NPs which force them to migrate towards the opposite polarity electrode	- Low consumption of sample and reagent - Fewer surface effect -More useful compared to Chromatography	- Time consuming	- Capillary electrophoresis (Ag, Au , inorganic oxides and CNTs) - Gel electrophoresis (DNA and RNA)	[8], [9], [10]
Size selective precipitation	- Based on difference in size , shape and surface coverage	- High efficiency ≥ 90%	- Most of the original sample will be discarded	- DNA induced size selective separation for Au NPs	[11], [12]
L - L Extraction	- Based on relative solubilities in two different immiscible liquids	- Ability to extract two or more different NPs in same time	--------	- Solvent extraction - Cloud point extraction	[13]
Field flow fractionation	- The dual effect of the flow behavior and field distribution in a thin open channel	- Small amount of samples in the ng-µg range - Parallel processing with multiple separation channels	- Sample preparation	- Magnetic field flow fractionation - Electrical field flow fractionation	[14], [15]

1.3 Separation and fractionation of nanoparticles in solutions by membranes

Filtration through a membrane is another alternative for the purification and size-fractionation of NPs. Membrane filtration has been used to separate or concentrate desired products via careful selection of the membrane pore size.

Ultrafiltration and nanofiltration membranes mostly cover the nanometer range. In 1996 IUPAC-nomenclature defines nanofiltration as the process of rejecting particles and dissolved molecules smaller than 2 nm and defines ultrafiltration as lying between 2 nm and 0.1 μm.[16]

Membrane-based filtration using media of a stated pore size has the following benefits; estimation of size-exclusion performance, easy scale-up by expanding the membrane area greener process that saves solvent during the purification and separation steps, convenient connections between processing tools such as reactors and analysis devices.[1]

Nowadays, using membranes for the fractionation and separtaion of nanoparticles is most widely used, because of the high efficiency and easy operation. By the same way, membrane separation and fractionation received high attention due to its environmental impact as it is considered as a green process. [7]

The work by Liang et al. [17], highlight the use of the carbonaceous nanofiber membrane for the filtration and separation of the nanoparticles. They demonstrated high efficient separation for three different types of nanoparticles Au, Ag, SiO2 using three membranes consisting of different size CNFs, namely, CNF-50, CNF-71, and CNF-98. Additionally, different particle were chosen for the testing i.e., 5, 25, and 60 nm Au, 25 nm Ag, and 150 nm SiO_2. The separations technique had been done by using batch dead-end mechanism.

The solution of binary mixture of Au nanoparticles 5 nm and 25 nm has volume of 14 ml in the ratio (2:12 ml) had been filtered with CNF-50. The retentate from this filtration process had been

dispered again in 20 ml of water for further filtration. Figure 1 is showing the results from the filtration process of the 25 nm Au nanoparticles solution.

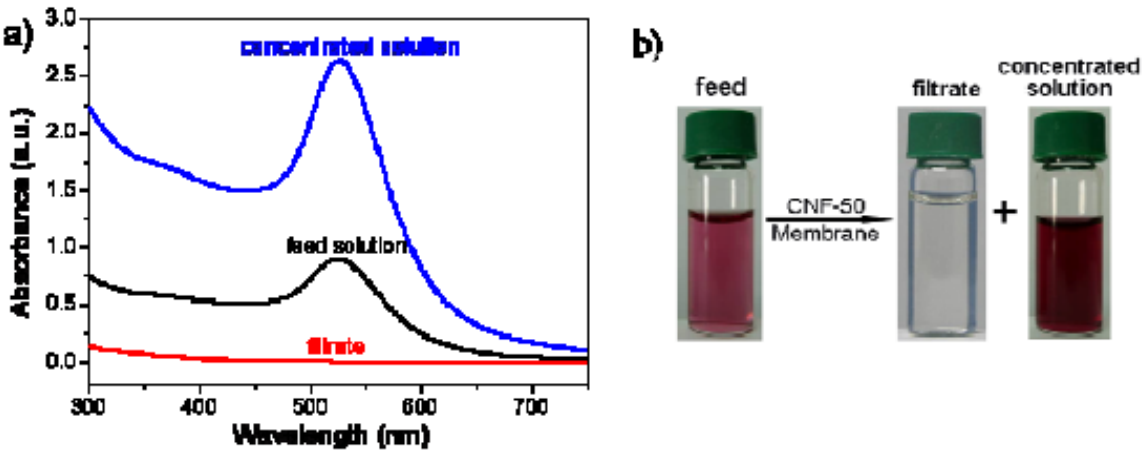

Figure 1: UV-vis spectra of the 25 nm Au nanoparticles feed solution, the concentrated solution and the filtrate permeated through the CNF-50 membrane. b) Optical images of the corresponding Au solution.[17]

Another mixture solution of Au had been separated with the CNF-71 and CNF-50 membranes successively. This mixture of volume 24 ml of mixed nanoparticle containing 5, 25, and 60 nm Au nanoparticles (4:8:12 mL). Three fractions; upper retentate on the CNF-71 membrane, middle retentate on the CNF-50 membrane, and the bottom permeate were collected and analyzed by TEM.

Figure 2 is showing the TEM analysis with a scale bar 200 nm for the mixed feed, the permeate and the retantae solutions from the separation process.

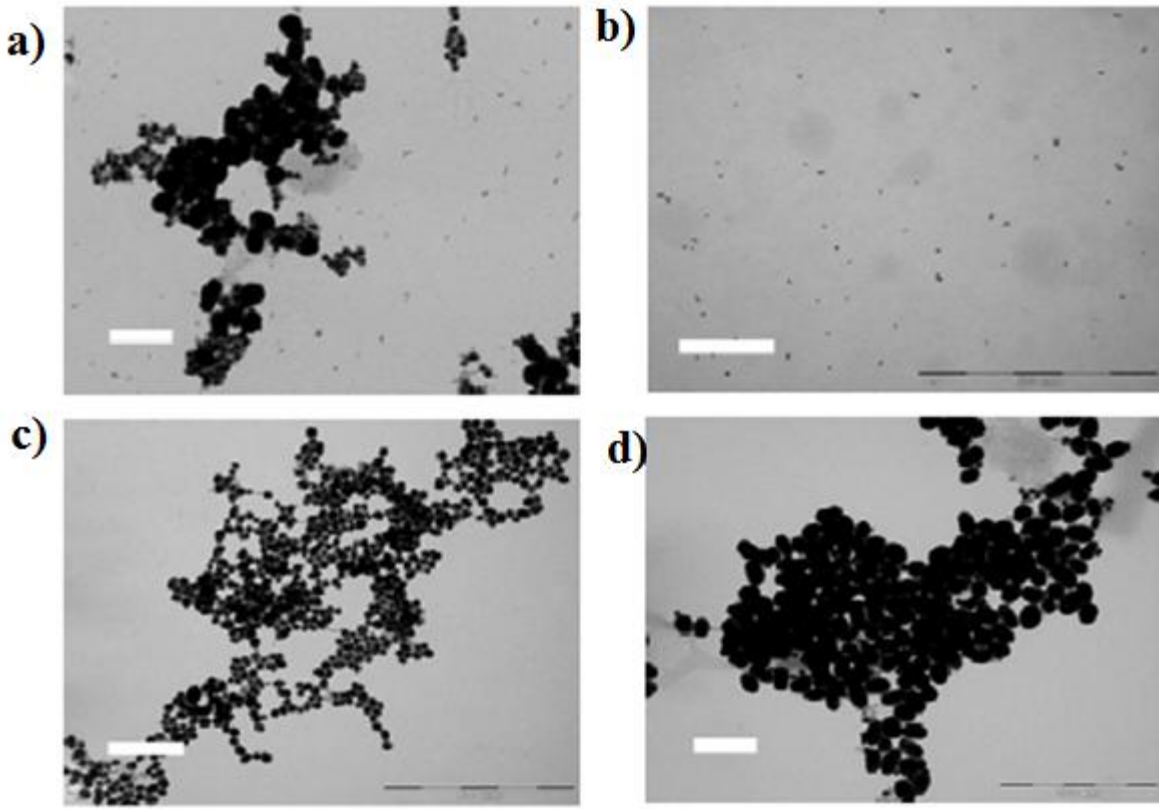

Figure 2: a) The original mixture consisted of 5 nm, 25 nm, and 60 nm Au nanoparticles. b) The bottom filtrate fraction permeated through the CNF-71 and CNF-50 membranes successively. c) The middle fraction retained on the feed side of the CNF-50 membrane. d) The upper fraction retained on the feed side of the CNF-71 membrane.[17]

On the other hand, another success has been obtained when Ag nanoparticles were tested with the CNF-50. The rejection of 25 nm Ag nanoparticles solution was almost 100%. Figure 3 is showing the UV-vis spectra for the feed and the filtrate solution.

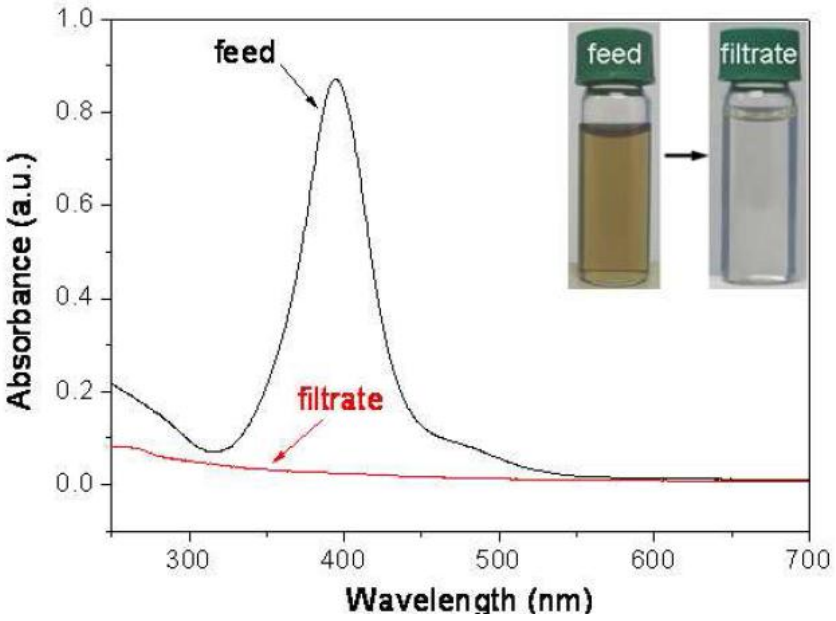

Figure 3: UV-vis spectra of the 25 nm Ag nanoparticles feed solution and the filtrate permeated.[17]

In the same work, silica nanoparticles solution with 150 nm diameter was filtrated using CNF-98 membrane. The filtrate had been characterized with SEM. Figure 4 is showing the SEM images for the silica nanoparticles solution before and after the filtration.

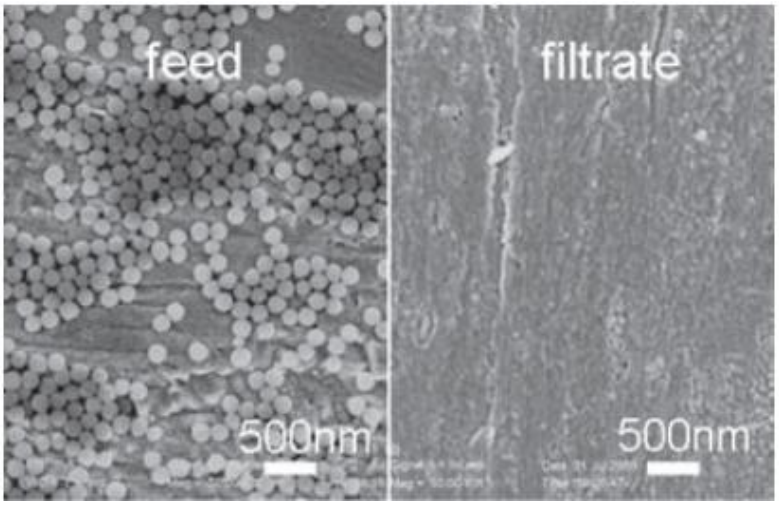

Figure 4: Filtration of 150 nm SiO 2 spheres using the CNF-98 membrane.[17]

Mekawy et al. [18] have studied using membrane in nanoparticles separation. In this work, Ag nanopaticles have a diameter in the range of 1-16 nm had been separated using trimethylsilyl (TMS) -silica hybrid (anodic alumina membranes) AAM membrane. Anodic Alumina Membrane (AAM) with pore size of 200 nm, diameter 2.5 cm, and thickness 60 µm was used. The separation system was based on size - exclusive of Ag nanoparticles. Figure 5A is showing the separated amount of Ag nanoparticles from this system, which was monitored by measuring UV–Vis absorbance after saturation AAM pores.

Additionally, it shows that 20% of the original amount of Ag nanoparticles could be separated in monodispersed and uniform Ag nanoparticles. However, the nanoparticles, with particle diameter larger than 4.5 nm, were blocked into the pore size or onto the surface of hybrid AAM as figure 5B and 5C is showing.

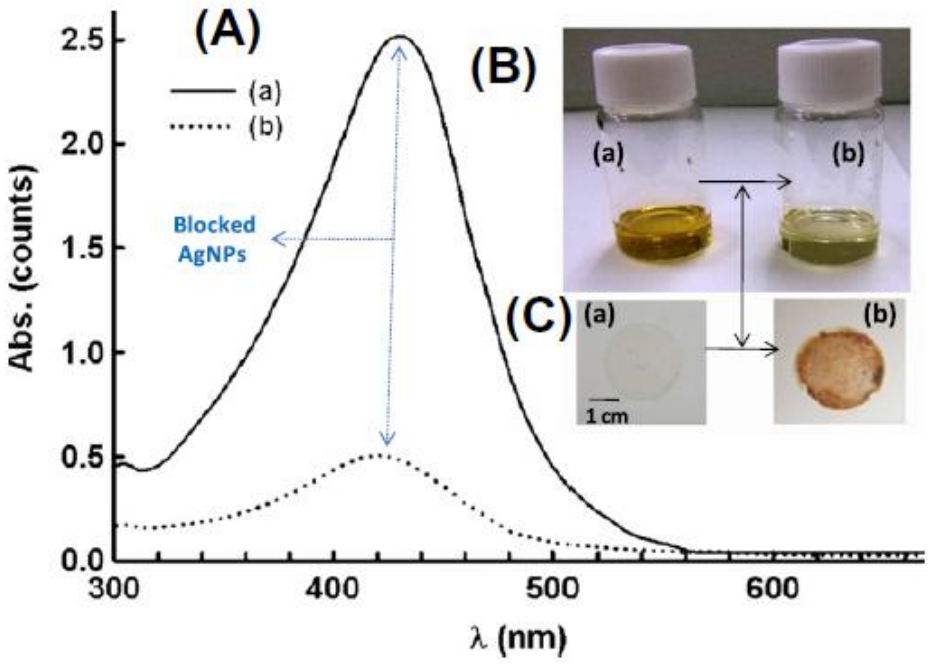

Figure 5: Absorbance spectra (A) of Ag NPs, and the color change of Ag NPs solution (B) and mesoporous TMS-silica hybrid AAM membranes (C) before (a) and after (b) filtration process.[18]

In addition, the separated Ag nanoparticles had been analyzed with high resolution TEM to show the effectiveness of the coated mesoporous TMS - silica hybrid AAM in the ultra fine separation of Ag nanoparticles.

Figure 6A is showing the HRTEM image and 6D showing the particles size distribution that the nanoparticles are spherical and irregularly shaped particles - for the Ag nanoparticles solution before separation. As same as the feed solution, the filtrated solution had been analyzed by TEM. Figure 6 (B-F) is showing the TEM analysis showed uniform spherical and regularly shaped particles with less than 4.5 nm in diameter, indicating the ultra fine separation of Ag nanoparticles by size and shape.

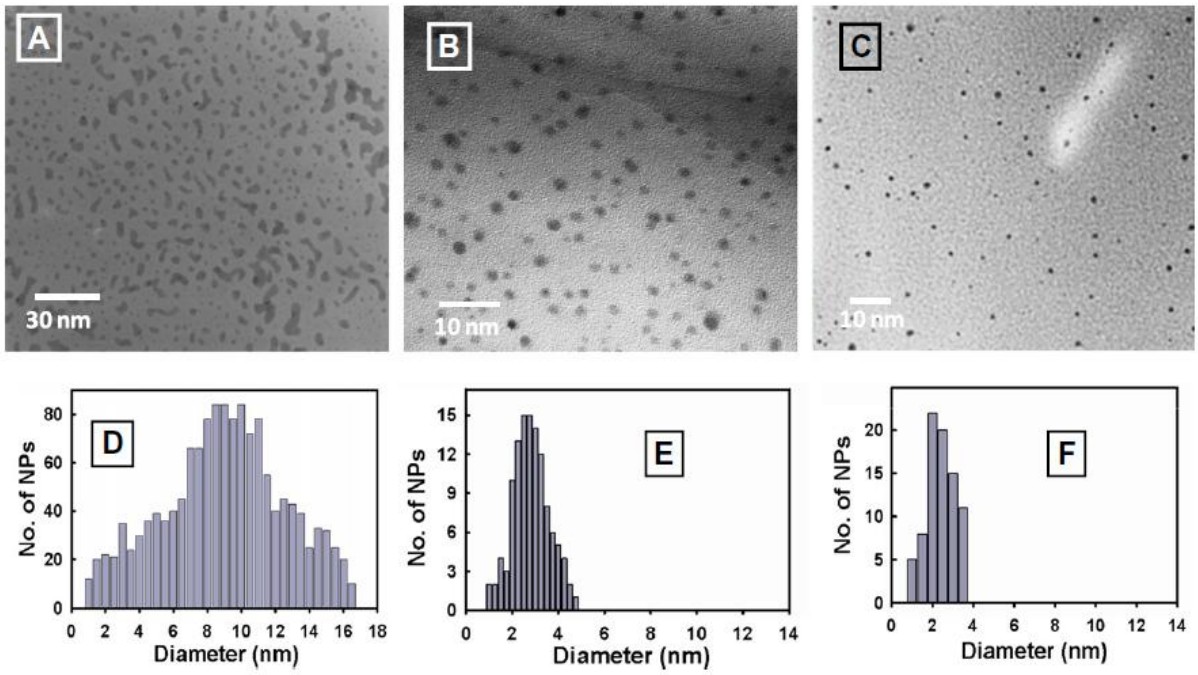

Figure 6: HRTEM micrographs of Ag NPs before (A) and after (B and C) application of size-based separation systems of mesoporous TMS-silica hybrid membranes and their representative histograms (D–F), respectively. [18]

Sweeney et al. [19] had demonstrated that membrane filtration is also a good method for the size-fractionation of water-soluble nanoparticles. The membrane which was used in this work is a poly(sulfon) diafiltration tubular membrane. They performed separate experiments in which they purified small Au nanoparticles (1.5 nm and 3.1 nm), separated binary mixtures into corresponding fractions, and finally fractionated polydisperse samples into several fractions characterized by different mean diameters of the metal cores. Figure 7 is showing the scheme of the continuous cross flow filtration setup used in these experiments.

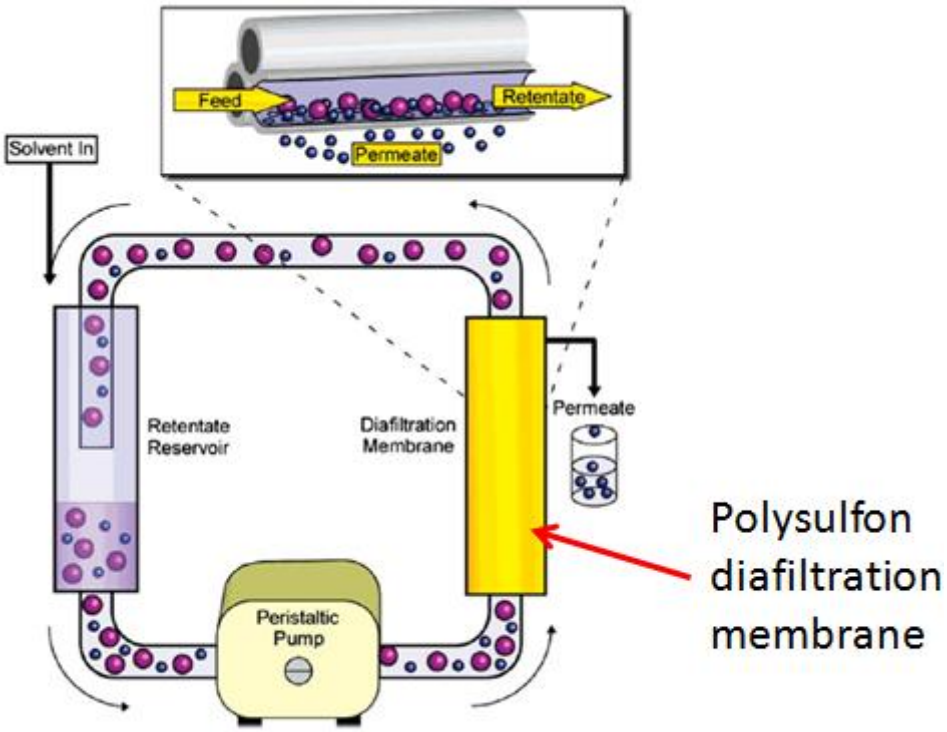

Figure 7: Scheme of a continuous filtration setup Sample and makeup solution are introduced into the retentate reservoir. The solution is pumped by a peristaltic pump through the filtration membrane. Small molecule impurities or small nanoparticles (blue) are eluted in the permeate, while the large NPs (purple) are retained. The expanded view illustrates a hollow-fiber-type filtration membrane eluting small impurities while retaining larger NPs.[19]

Briefly, a water-based NP sample was placed in a reservoir, from which it was drawn by a peristaltic pump into the filtration membrane. The rate of water addition to the reservoir was adjusted to match the rate of elution. Filtration was continued through multiple filtration volumes until reaching the desired rate of size separation or sample purity.

In this work, a binary mixture of Au nanoparticles 1.5 nm and 2.9 nm with a ratio in 1:1 had been filtered with 10×15mL of water through 50 kDa membrane (nominal molecular weight cutoff, MWCO, wherein a 50 kDa means the membrane will retain 90% of a globular protein with a molecular mass N50 kDa).

The quality of separation using diafiltration membrane had been determined by TEM and UV-vis. Figure 8 is showing the TEM and UV-vis analysis which showed that retained fraction comprised 2.9±1.0 nm nanoparticles, while permeate had 1.5±0.5 nm sized particles and the data were compared to those for Au3.1-70R, Au1.5-10R, and Aux-mix.

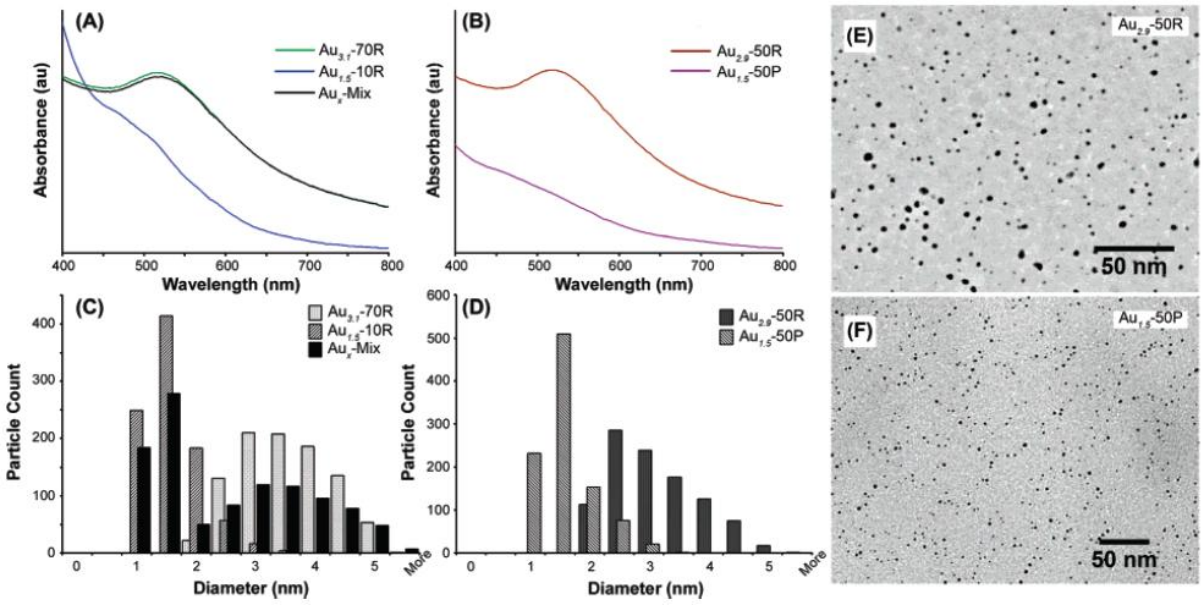

Figure 8: (A) UV-vis spectra for the initial samples Au3.1-70R and Au1.5-10R and the mixture Aux-mix. (B) UV-vis spectra of the separated fractions Au2.9-50R and Au1.5-50P. (C) Stacked TEM histograms for the initial samples Au3.1-70R and Au1.5-10R and mixture Aux-mix. (D) Stacked TEM histograms for the separated fractions Au2.9-50R and Au1.5-50P. (E, F) Representative TEM images of the separated fractions Au2.9-50R and Au1.5-50P.[19]

Finally, these authors have shown that a sample containing polydisperse nanoparticles could be fractionated using membranes characterized by different MWCO values. Figure 9 is showing that in their work, the initial solution had been first filtered through a 70 kDa membrane which retained the largest, 2.9±0.9 nm, particles. The remaining permeate had been then filtered through a 50 kDa membrane, and the retained particles had been again collected; these particles had a size distribution 2.6±0.9 nm. Smaller range of nanoparticles had be retained by repeating the separation process with small membranes 30 kDa and 10 kDa (2.5±0.9 nm and 2.0±0.7 nm, respectively).

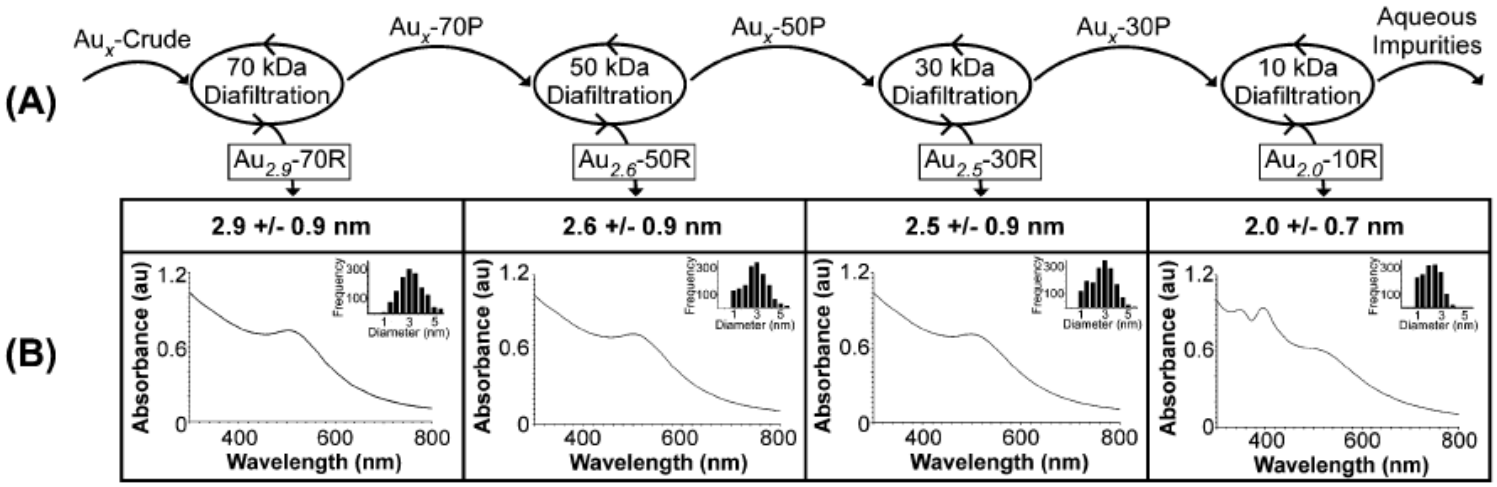

Figure 9: (A) Diafiltration scheme used for obtaining nanoparticle fractions. Following each diafiltration step, the retentate is analyzed via UV-vis and TEM and the permeate is further diafiltered on a smaller MWCO membrane. (B) Summary UV-vis and TEM data for each fraction. With each decrease in pore size, the average core size decreases, with corresponding blue shifts and broadening of the plasmon resonance peak in the UV-vis spectrum.[19]

As a conclusion from the published work, as in [17] a batch dead end process Au NPs, Ag Nps having particle diameter 25 nm have been filtrated using CNF-50 membrane with a rejection almost 100%. In addition, solution of silica NPs have particles diameter 150 nm had been rejected with the CNF-98 with a rejection value ≥ 99 %.

By the same way, Ag NPs in the range of 1-16 nm have been separated and filtrated using trimethylsilyl (TMS) - silica hybrid membrane[18]. The previous separation process had been done using cross flow method of separation. Additionally, 20% of the original amount of Ag nanoparticles could be separated in monodispersed and uniform Ag nanoparticles.

And last but not least, the separation and fractionation of Au NPs had been succeed. Using the polymeric membrane in cross flow filtration method, the final Au NPs from the fractionation process has a particle diameter 2.0±0.7 nm after passing through different MWCO membrane.[19]

These results will be taken in consideration in order to be compared with the results obtained from the filtration and fractionation processes, which will be done in this work.

Chapter two: Objective

The goal of this thesis is to evaluate commercial ceramic membranes for fractionation and separation of nanoparticles. In order to achieve this goal several sub objectives have been accomplished.

(i) Synthesis of silica nanoparticles using different procedure producing nanoparticle with different range of diameter and with different polydispersity.

(ii) Synthesis of silver nanoparticles aiming to produce nanoparticle with a diameter in the range of 5-30 nm.

(iii) Design a simple experimental set-up for the different filtration modules dead end and cross flow filtration.

(iv) Separate and filtrate the nanoparticles solution of different concentrations using the commercial membrane and the designed experimental set-up.

(vi) During all the previous steps; all the synthesized nanoparticles and solutions before and after filtration will be characterized by the appropriate techniques.

Chapter three: Experimental work

3.1 Chemicals

Ethanol (C_2H_6O) with molecular weight 46.07 g/mol and purity 99.8% and ammonia withmolecular weight 17.03 g/mol and concentration 25% - were purchased from PanReac . Inc. (Barcelona, Spain). Tetraethyl orthosilicate ($C_8H_{20}O_4Si$) with molecular weight 208.33 g/mol and purity 98% - , ethylene glycol ($C_2H_6O_2$) with molecular weight 62.07 g/mol and purity ≥99 % - were purchased from Sigma Aldrich (Laborchemikalien GmbH, Seelze, Germany). Ammonium hydroxide withmolecular weight 35.05 g/mol and concentration 28% was purchased from Sigma-Aldrich Quimica SL (Madrid, Spain). Polyvinyl pyrrolidone $(C_6H_9NO)n$ with molecular weight 10000 g/mol - and Silver nitrate ($AgNO_3$) , molecular weight 169.87 g/mol and purity 99.999 % - were purchased from Sigma Aldrich (St. Louis, Missouri, USA).

3.2 Membrane

Ceramic membranes were used in this study were Inopor®nano (inocermic GmbH, Hermsdorf, Germany) membranes. Two different pore sizes membranes had used for separation and fractionation process. Both ceramic membranes were used in this study membranes had an outer diameter 5 mm and an inner diameter of 3 mm and thickness of 1 mm. These membranes are asymmetric with a mean pore size of 5 nm and 60 nm.

Both membranes had been cut to small membrane with 4.5 cm length. The filtration length was controlled to be 2.5 cm by enameling both ends to totally block the pores of the ends of the sectioned membranes. Thereafter, calcinations step had been done, in the calcinations step the polished membrane had been introduced to a high temperature oven at 850 ^oC for 1 hr. The membrane after calcinations step would have a shiny ended.

A) Titania membrane

With reference to the smaller pores size membrane, the active membrane layer was composed of Titania (TiO2), which was deposited on a coarse-porous support Alumina (Al2O3). The whole thickness of the membrane is 1 mm. While the thickness of the small particles and pores layers was 60 µm and the rest was the big pores and coarse alumina support layer. The alumina support layer was divided to four layers with different thickness Coarseness and particles size.

Figure 10 shows the scanning electron microscope image of the whole membrane thickness and the thickness and the structure for each layer separately. As shown in the images, the titania layer has a thickness around 600 nm and the four different alumina layers have thickness around 940 µm, 14.4 µm , 25 µm and 20 µm for the bigger pores and coarser particles to the smaller pores and finer particles respectively.

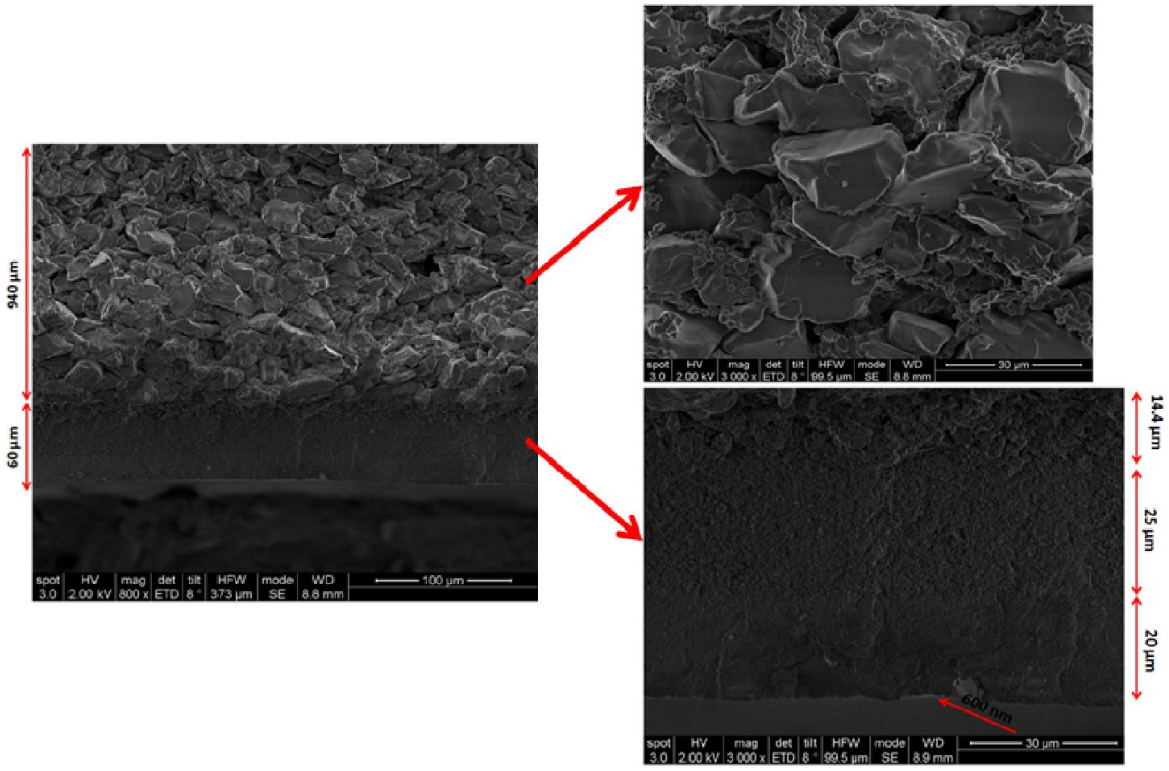

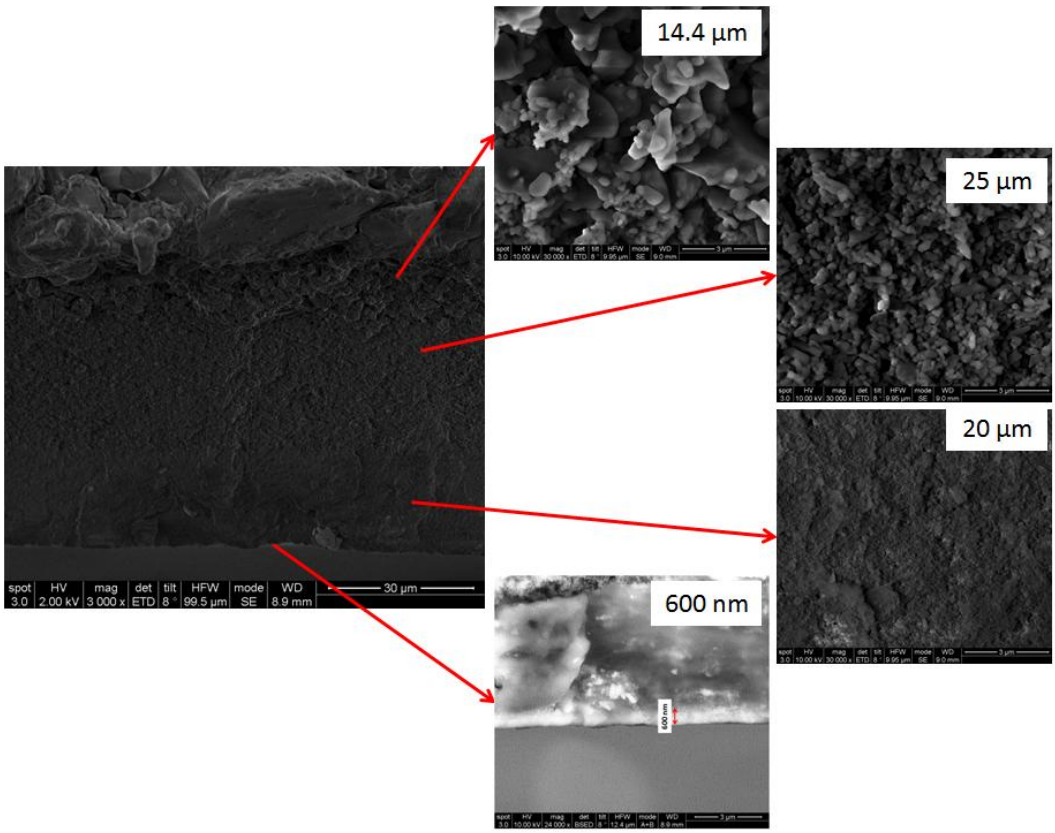

Figure 10 : SEM image for TiO_2 membrane

B) Alumina membrane

On the other hand, the 60 nm pores size membrane was an alumina membrane. The 1 mm thickness of this membrane is divided to four layers as same as the smaller pores size membrane but without the titania layer. The thicknesses of the four layers are 940 µm, 15 µm, 25 µm and 20 µm from the coarser to the finer layer respectively. Figure 11 is showing the scanning electron microscope image for the whole 60 nm pores membrane thickness.

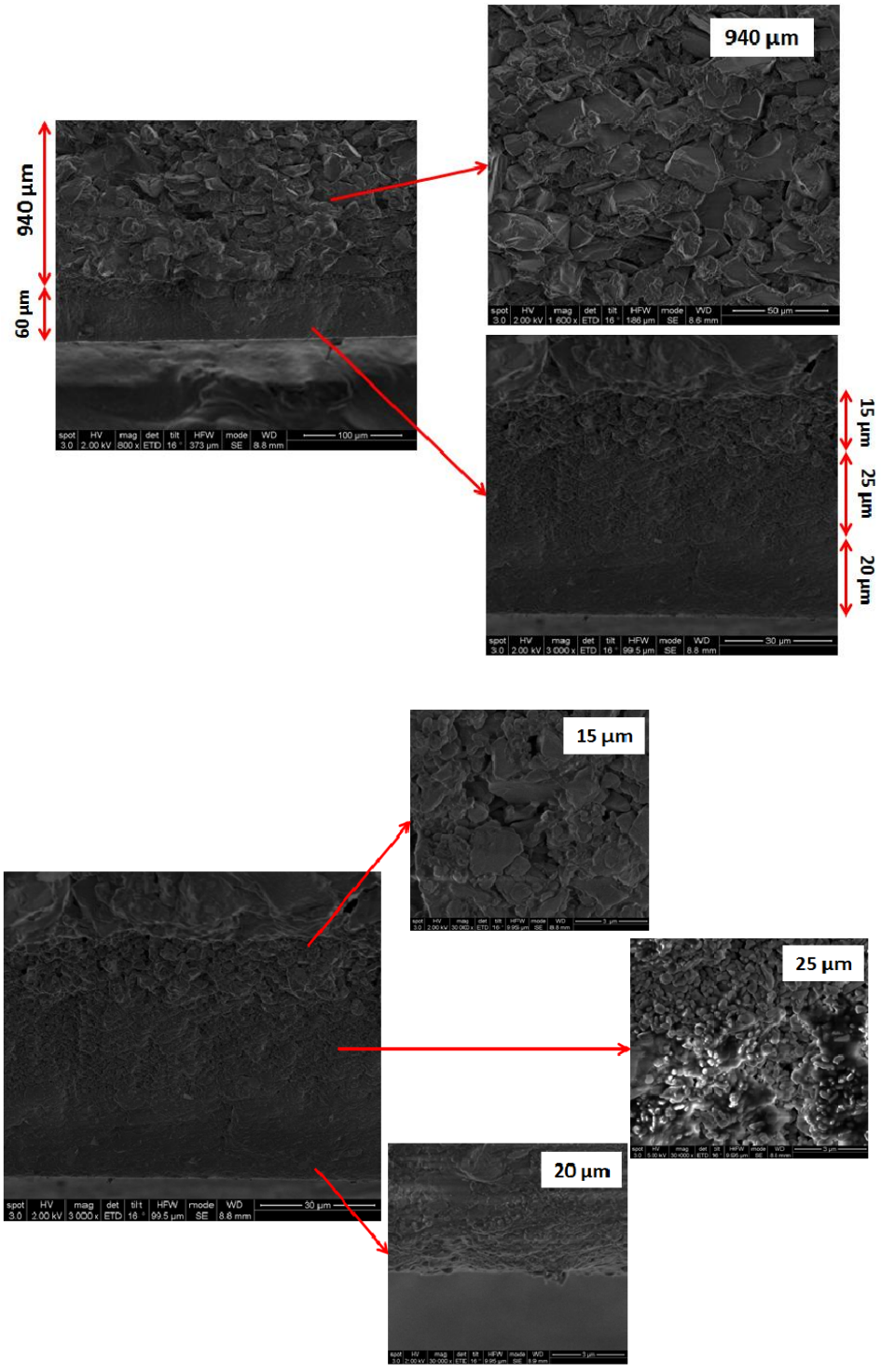

Figure 11 : SEM images for alumina 60 nm pores membrane characterization.

3.3 Nanoparticles synthesis procedure

3.3.1 Synthesis of silica nanoparticles

The Stöber process [20] is used for the preparation of monodispersed silica colloids by means of hydrolysis of alkyl silicates and subsequent condensation of silicic acid in alcoholic solutions using ammonia as catalyst. The diameter of silica particles from this process is controlled by the relative contribution from nucleation and growth processes.

The hydrolysis and condensation reactions provide precursor species and the necessary supersaturation for the formation of particles. During the hydrolysis reaction, the ethoxy group of tetraethyl orthosilicate "TEOS" reacts with the water molecule to form the intermediate (Si $(OC_2H_5)_4$-X (OH)X) with hydroxyl group substituting ethoxy groups. Ammonia/ammonium hydroxide works as a basic catalyst to this reaction; the hydrolysis reaction is initiated by the attacks of hydroxyl anions on tetraethyl orthosilicate "TEOS" molecules [21].

Two procedures of the silica nanoparticles were performed based on Stöber method to produce polydisperse and monodisperse silica nanoparticles. The difference between both procedures is the amount of the precursor and the amount of catalyst. The molar composition between tetraethyl orthosilicate: ammonium hydroxide is as following 1:1 in the ultrasonic method and 1: 2 for the conventional stirring method.

A) Ultrasonic method

The synthesis procedure was as follows: 4 ml of tetraethyl orthosilicate "TEOS", 50 ml of ethanol and 4 ml of ammonium hydroxide 28% were taken. The mixture of ethanol and tetraethyl orthosilicate "TEOS" was stirred for 2 minutes, and then the ammonium hydroxide was added to the mixture during the stirring process to make sure of completely mixed solution. The mixture after the stirring process had been inserted to ultrasonic bath for 2 hr at room temperature. In the last mentioned step, the silica nanoparticles must have already been synthesized.

B) Conventional Stirring methods

The synthesis procedure was as follows: 50 ml of ethanol, 3 ml of ammonium hydroxide 28-30% and 1.5 ml of tetraethyl orthosilicate "TEOS" were taken. The mixture of ethanol and ammonium hydroxide was stirred for 2 min and during stirring the tetraethyl orthosilicate "TEOS" was added drop by drop very slowly. The mixture then had been stirred for 1 hr or until the solution color start to be converted from clear transparent solution to milky turbid solution at temperature 30^{o}C .[22]

Thereafter for both methods, the mixture was centrifuged at 10000 rpm for 10 min to separate the synthesized particle from the colloidal solution. For finishing the synthesis, the silica nanoparticles were washed by absolute ethanol for three times to remove non-reacted tetraethyl orthosilicate "TEOS". The solution after washing by using ethanol has been washed by deionized water to prepare the solutions for filtration.

3.3.2 Synthesis of silver nanaoparticles

Silver nanoparticles had been synthesized by microwave assisted polyol synthetic approach. The microwave-polyol method is a promising method for the rapid synthesis of rods, wires, polygonal plates, sheets, and dendrite types of silver nanostructures. Yamamoto et al. [23] prepared triangular Ag nanoplates by using microwave promoted reduction of silver nitrate "$AgNO_{3}$" in aqueous solutions involving polyvinyl pyrrolidone "PVP". In the other hand, by using the microwave polypl method only spherical Ag nanoparticles were prepared by Pal et al.[24] .

Ehylene glycol "EG" acts as a reducing agent as well as a solvent with a high boiling point of 198 ^{o}C, and high reduction ability. Since ethylene glycol "EG" has a large dielectric loss constant of 41.0, it is an ideal solvent in microwave heating synthesis of metallic nanostructures.

Polyvinyl pyrrolidone (PVP, Mw: 10,000), silver nitrate (99,9999%) , ethylene glycol (anhydrous, 99 %) and deionized water were used to prepare aqueous solutions. First, 20 ml of

ethylene glycol "EG" was transferred to a glass beaker and was stirred with a magnetic stirrer. While stirring 2.4 g of polyvinyl pyrrolidone "PVP" was added slowly to the solution.

The solution was covered and stirred for 2 hr. An amount of 0.158 g of silver nitrate "$AgNO_3$" powder was added to the solution. The beaker was then covered with aluminium foil to protect it from the light, as the silver is a photosensitive material.

The mixture of silver nitrate, polyvinyl pyrrolidone and ethylene glycol was then agitated continuously for 20 minutes. The mixture was then subjected to microwaves in order to synthesize the nano-spheres of specific diameters.

In the CEM discover single-mode microwave which was enabled with Synergy program SintNPsAG23s which exposing the mixture to 23 seconds at 2 00 Watts of power and maximum temperature of 200^0C, which intern synthesized spheres of diameters 5-30 nm in diameter.

The sample temperature was monitored by an optical fibber immersed in the reaction mixture. Thereafter, the resulting solution was cooled rapidly in an ice bath. The mixture then was transfered to centrifugal tubes to introduce it to the centrifuge. The tubes were subjected to centrifugation at 21000 rpms for 1 hour; this process is repeated 6 times. In the first 5 times 10 ml of the supernatant was removed and replaced with a fresh deionized water. While in the sixth wash almost all the supernatant was removed and replaced with fresh deionized water.

3.4 Experimental set-up

3.4.1 Filtration/Separation methods

Filtration processes are defined as dead-end or cross-flow by the solution stream direction. In this study, both filtration processes had been used with the silver and silica nanoparticles separation. Figure 12 is showing a schematic for both techniques.

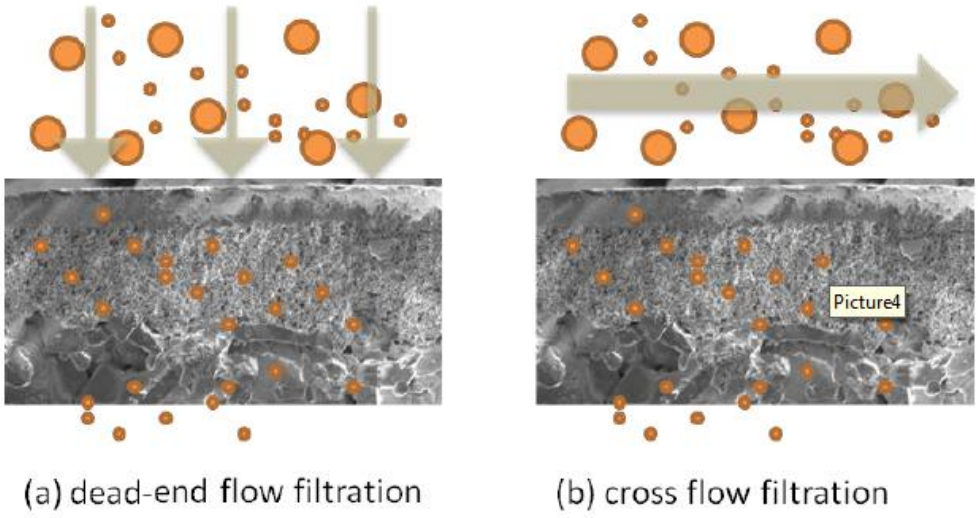

Figure 12: Separation mechanism ; (a) dead-end flow filtration, (b) cross-flow filtration.[1]

a) Dead-end process

The most basic form of filtration is dead-end filtration. The feed suspension flows perpendicularly to the membrane. Any particles in the feed solution that are larger than the pore size of the membrane are accumulated on the membrane surface forming a cake of solids and the rest of particles which are lower size than the pore size is passing through the membrane . The solution, which passed through the membrane, is called filtrate.

The accumulated particle" cake" on the surface of the membrane decreases the filtration rate due to clogging. In spite of the flushing step had to be done after each batch to remove the filtrate cake and clean the membrane surface, in case of low concentrated solutions, dead end process is the most useful technique for concentrating compounds.[25], [26]

b) Cross-flow process

In cross-flow filtration, the flow direction is parallel to the membrane surface and the feed flow and filtration flow direction have a 90 degrees angle. The feed flow through the membrane has an elevated pressure as driving force for the filtration process and a high flow speed to create turbulent conditions.

This set-up has proved effective in reducing the clogging of membrane pores because of the turbulent flow along the membrane surface, which prevents the accumulation of matter on the membrane surface. In addition, this technique is scalable method that allows continuous-flow operation.

The outlets from this technique are two streams: a permeate stream (or filtrate stream) which is perpendicular on the feed and a retentate stream, which flows tangentially to the feed stream.[26], [27]

3.4.2 Set-up

A simple experimental set-up have been designed in the laboratory. Using SHIMADZU LC-10AT$_{VP}$ High Performance Liquid Chromatography (HPLC) pump connected to stainless steel connections to introduce the solution to the membrane. Pressure was measured using pressure meter. Figure 13.a, 13.b, 13.c showing the experimental set-up for both separation/filtration technique cross-flow, dead-end and the backwash set-up respectively.

The needle valve in the cross-flow set-up was used to control the retentate amount and the plug in the backwash and the dead-end was for blocking the other side from the membrane and force the solution to go through the opened side of the membrane.

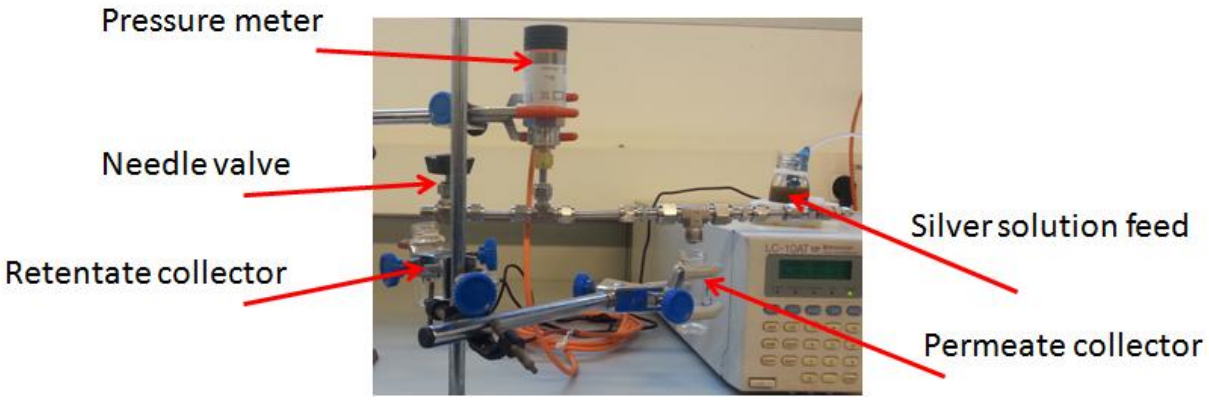

(a)

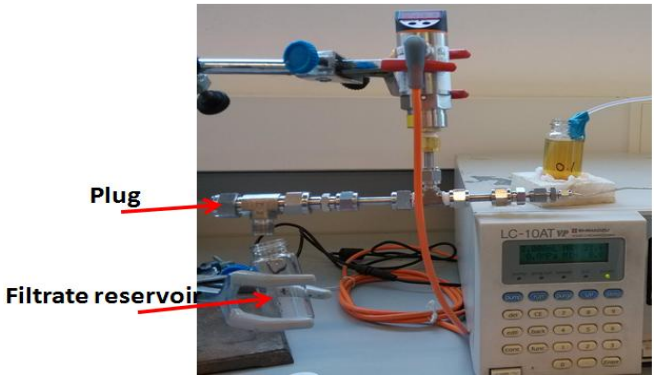

(b)

(c)

Figure 13 : Experimental set-up simple design.

3.5 Characterization and analysis Methods

In order to analyze the produced nanoparticles and characterize the results; before and after filtration/ separations, particles size, concentration, structure, yield had been measured. The particles samples were characterized carefully using the following techniques:

Dynamic light scattering (DLS) particle size analyzer for particle size distribution, Scanning Electron Microscopy (SEM) for the silica nanoparticles and Transmission Electron Microscopy (TEM) for the silver nanoparticles to reveal their formation and corresponding morphologies, Micro-balance for concentration and yield measurements and finally Ultraviolet visible (UV-vis) scanning spectrophotoscopy to detect the distinct spectrum of the silver nanoparticles produced. Microwave coupled plasma atomic emission spectroscopy (MCP-AES) had been used additionally to distinguish quantitatively the amount of silver in the final product.

3.5.1 Dynamic Light Scattering - DLS

Dynamic light Scattering is also known as photon correlation spectroscopy (PCS) or quasielastic light scattering (QELS). This technique is based on measuring the Brownian motion by collecting the scattered light from suspended particles to obtain diffusion rates to calculate their particle size. [28]

As the particle size can be determined by measuring the random changes in the intensity of light scattered from a suspension or solution. The samples solutions were introduced to the Brookhaven 90 (Brookhaven Instruments Corp.) photo correlation spectroscope. The result from DLS could give an overview about the sample polydispersity through the polydisperse index.

In particular, few drops of the samples was subjected to the measurement cubit and was diluted with fresh deionized water. Each sample was measured during six runs and each was 3 minutes. The results had been graphed using Origin software.

In addition, non-linear curve fitting (Gauss) had been graphed to calculate the mean diameter- which is giving in terms of the center of the peak- of the sample , value of quantifies goodness of fit (R^2) and the full width at half maximum (FWHM). The full width at half maximum (FWHM) value, is typically depending on the polydispersity of the sample.

3.5.2 Scanning Electron Microscope - SEM

As scanning electron microscope is one of the most used in the entire electron microscopy instrument. Scanning Electron Microscopy (SEM) was the second technique used to obtain information about the particle size and morphology of the nanoparticles.

Scanning electron microscopy images were obtained with (Oxford instruments, INCA PentaFET-x3). The nanoparticles were prepared in the solid powder phase to be viewed by the SEM. The sample preparation was as follows: one drop the sample was poured on a glass sheet and dried at atmospheric temperature over the night. The sample powder was then scratshed using a laboratory spatula. Finally, the powder was fixed to the SEM sample holder using a carbon tap. As the powder should be homogenously distributed on the sample holder, the powder was smashed again.

The images were obtained using the ETD and the Secondary electron imaging mode. Due to the resolution of the SEM and the particles size of the nanoparticles , only silica nanoparticles has been viewed with.

3.5.3 Transmission electron microscopy - TEM

The transmission electron microscopy can yield information such as particle size, size distribution and morphology of the nanoparticles as well as dispersion uniformity at the nano-scale.

In this work, according to the TEM higher resolution compared with the SEM , TEM had been used to analyze the silver nanoparticles which particles size in the range of 5- 30 nm.

Transmission Electron Microscopy images were obtained with a FEI Technai T20 (LTEM) transmission electron microscope.

A thin layer of the dried silver nanoparticle was prepared by depositing one drop of the sample solution on a carbon grid and dried over the night in atmospheric temperature. Based on the difference in the atomic density, the electrons will pass through the grid faster than the silver nanoparticles. The electron sensor identifies the silver nanoparticles with the high density and represents them as dark areas. In some cases, the excess of the polyvinyl pyrolidone, which hadn't removed during the washing steps, could appear as lighter areas.

3.5.4 Ultraviolet–visible spectroscopy - UV-vis

Silver is a metal nanoparticle, so the conduction band and valence band lie very close to each other in which electrons move freely. These free electrons give rise to a surface plasmon resonance (SPR) absorption band, occurring due to the collective oscillation of electrons of silver nanoparticles in resonance with the light wave. [29]

Ultraviolet–visible spectroscopy absorption spectra have been proved to be quite sensitive to the formation of silver colloids because silver nanoparticles exhibit an intense absorption peak due to the Surface Plasmon excitation. The absorption spectrum of isolated spherical particles is characterized by the Mie resonance. The absorption band in visible light region (350 nm – 550 nm), Plasmon peak at (400 nm - 420 nm) is typical for silver nanoparticles.[30]

According to the previous information, the solution of the silver nanoparticles had been analyzed using Ultraviolet–visible spectroscopy measuring the wavelength in nanometer versus the absorbance. The Ultraviolet–visible absorption peaks, which were characterized in this work, were measured by using a Hellmanex JASCO V- 670 spectrophotometer.

The measurements were obtained in the wavelength range of 250-850 nm as first and last wavelengths. The number of measured points was set to be 551 point. The Ultraviolet–visible absorption peaks for the first, the sixth removed supernatant and for the sample after few days of

synthesis had been obtained in order to observe the existence of silver nanoparticles in the removed supernatant and oversee the effect of time after synthesis on the stability of the silver nanoparticles.

3.5.5 Microbalance - Concentration and yield measurements

In order to estimate the conversion of the reactant to produce the nanoparticles or having an idea about the mass balance of the filtration / separation process . The concentration for each sample was measured and the yield of the reatcion was calculated.

In addition, after the separation process the concentration of the filtrate in the dead-end process and the permeate and the retantate for the cross-flow process were measured .

In particular, the concentration was measured by using RadWag microbalance. The measurement had done by the following procedure: different volumes from the sample were inserted in small cubit ,which is designed especially for this measurement. Thereafter, the aluminum cubit was covered with its cover and compressed to be totally closed.

Small opening was done in the surface of this cover to allow the solvent evaporation through it. The small cubit was then subjected to conventional oven to evaporate the solvent. As in this case, the solvent is water so convention oven at 90 ^{o}C was used to evaporate the solvent in duration from 2-3 hours.

The weight of the covered cubit had been measured before and after evaporation of the solvent. The difference in the weight represents the mass of the nanoparticles inside the cubit. The difference in the weight had been graphed verses the volume which introduced in each cubit. The slope of the fitted line through these points is the concentration of this sample.

Table 2 : Concentration measurement for silver nanoparticles using RadWag microbalance.

Volume (µl)	Volume (ml)	M1(mg)	M3(mg)	delta M (mg)
30	0.03	49.858	49.94	0.082
40	0.04	80.059	80.155	0.096
50	0.05	80.421	80.537	0.116
60	0.06	79.979	80.111	0.132

The results n table 2, represent the volume of the sample which was inserted in each cubit in microliter and its conversion to milliliter (Volume). While M1 and M2 represent the weight of the cubit before and after evaporation and delta M is the difference between them. Figure 19 is showing, plotting these data and the linear fitting for them. As shown in the figure, the slope of the line is 1.7, which represents the concentration in mg/ml.

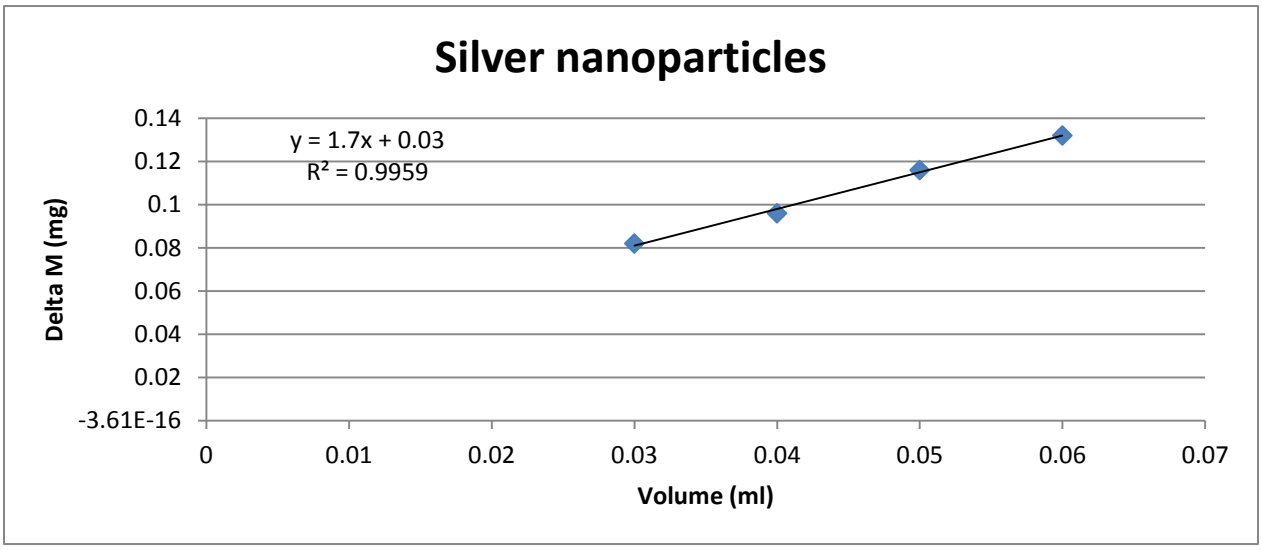

Figure 14: Concentartaion measurment.

Furthermore, the yield was calculated using the concentration , volume and the molecular weight of each component.

Amount of $AgNO_3$ in = 158 mg

Amount of Ag in

$$= Amount\ of \text{ silver nitrate } in * \frac{Molecular\ weight\ of \text{ silver}}{Molecular\ weight\ of \text{silver nitrate}}$$

$$=158\ mg * \frac{107.86\ mg * 1\ mmol}{1\ mmol * 168.87\ \text{mg}} = 100.97\ \text{mg}$$

Amount of $AgNO_3$ out

$$= \quad Volume\ of\ sample(ml) * Concentraion(\frac{mg}{ml})$$

$$= 31\ (ml) * 1.7(\frac{mg}{ml}) = 52.7\ \text{mg}$$

Amount of Ag out

$$= Amount\ of \text{ silver nitrate } out * \frac{Molecular\ weight\ of \text{ silver}}{Molecular\ weight\ of \text{ silver nitrate}}$$

$$=52.7\ mg * \frac{107.86\ mg * 1\ mmol}{1\ mmol * 168.87\ \text{mg}} = 33.66\ \text{mg}$$

Yield %

$$= 100 * \frac{Amount\ of\ silver\ out}{Amount\ of\ silver\ in}$$

$$=100 * \frac{33.66}{100.97} = 33.35\ \%$$

With similar measurements of the concentration and calculations of the yield, the concentrations and yields had been measured and calculated for all the samples of both nanoparticles silica and silver nanoparticles before and after the filtration process. In addition to the yield calculations, the % of rejection for each membrane had been calculated based on the concentration as the % of rejection value is given by the following equation [26] :

$$\text{Rejection value} = \left(1 - \frac{Concentration\ of\ the\ permeate/filtrate}{Concentration\ of\ the\ feed\ solution}\right) * 100$$

5.3.6 Microwave coupled plasma atomic emission spectroscopy (MCP-AES)

Microwave coupled plasma atomic emission spectroscopy (MCP-AES) also referred to as microwave coupled plasma optical emission spectrometry (MCP-OES). MCP is an analytical technique used for the detection of trace metals. Basically,it had been used to distinguish quantitatively the amount of silver in the final product after the filtration / separation process.

The filtrate and the backwash concentration from the dead-end process for the low concentrated silver nanoparticles solution had been observed using Agilent Technologies, 4100 MP-AES. The measurement of the samples should be preceded by calibration.

Using a standard samples of known concentration 1, 3, 5, 7, 9 ppm of a standard silver solution with the addition of aqua regia (HNO_3: 3HCl) and fresh deionized water in the ratio 1: 3 . In addition, a blank sample had been prepared without addition of the silver slandered as a reference for the following measurements.

The samples had been prepared in the same conditions of the patrons and the ratio between sample: water: aqua regia was 1:3:1. The measurement had been done at two wavelengths 328 and 338 nm. The measurement had been repeated twice to ensure the results for each sample and in the end the value of the concentration will be estimated from the average of these two measurement at the different wavelength.

Chapter four: Results and discussion

4.1 Nanoparticles synthesis and their characterization

4.1.1 Silica nanoparticles characterization

Four different batches had been prepared using the ultrasonic procedure and three using the conventional stirring method. All the batches had been characterized using the Dynamic Light Scattering (DLS) and the Scanning electron microscope (SEM).

4.1.1.1 Ultrasonic Procedure

A) Dynamic Light Scattering

As discussed in the previous chapter, the DLS results had been plotted using Origin software .In addition some samples' results had been fitted with the Gauss non-linear fitting to observe the mean diameter of the nanoparticles.

Results in table 3 show that the ultrasonic procedure for synthesis silica nanoparticles is non-reproducible in terms of nanoparticles size, concentration, and the synthesis yield. The temperature of the ultrasonic bath and the exact position of the synthesis mixture could be the main reasons for the non-reproducibility of this procedure. As the temperature changing from one position to another inside the ultrasonic bath, this could affect on the conversion of the reaction and consequently the concentration and the yield could be changed conversely.

On the other hand, from the polydipersity point of view the ultrasonic procedure is giving a monodisperse distribution of nanoparticles as the result of the polydispersity index show for the all batches.

Table 3: DLS characterization for 4 batches of silica Synthesis using Ultrasonic

Sample/ Data	1	2	3	4
Mean Diameter (nm)	188	226.5	381.4	145.2
Mean Diameter fitting (nm)	140.53	No fitting	No fitting	140.25
FWHM (nm)	19.2	No fitting	No fitting	54.7
PDI	0.084	0.059	0.005	0.063
Concentration (mg/ml)	20.56	5.7	15.64	8.34
Yield (%)	91.8	79.54	90.94	31.8
PH	9.48	9.07	9.15	8.77

Figure 15 (a-d), is representative for the 4 batches plotted and the fitting curves for some of them respectively. As shown in figure 15 for batch 1 and 4, the Gauss non-linear fitting curve is in red color while the main distribution from DLS is in the black color.

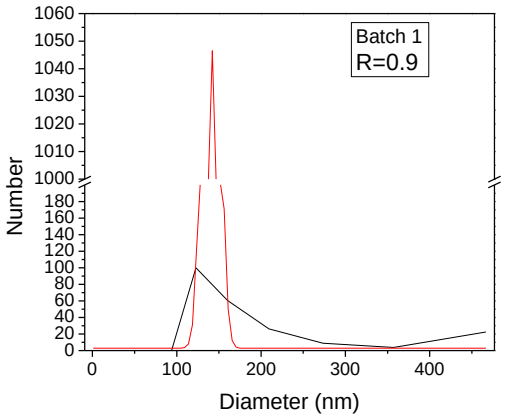

(a)

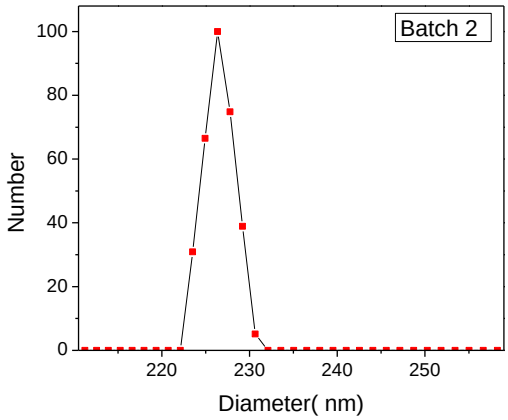

(b)

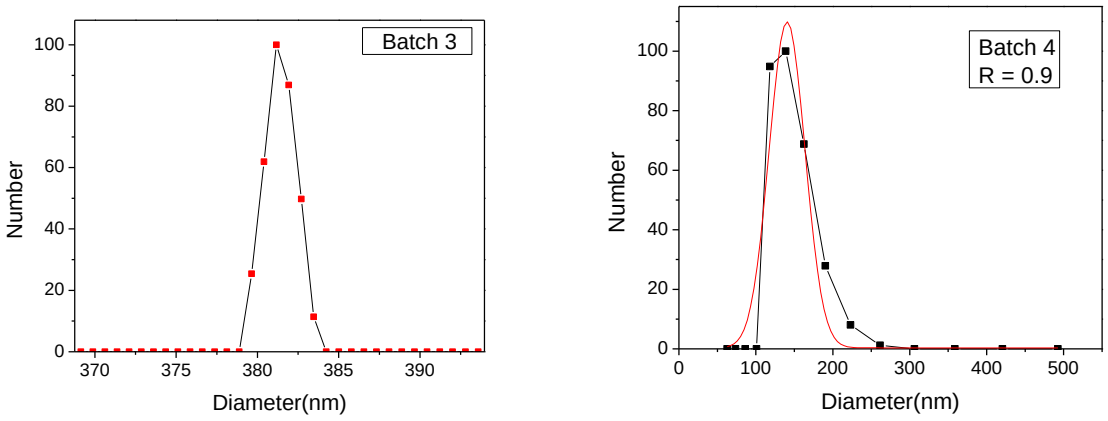

(c) (d)

Figure 15: DLS characterization for the four samples; (a), (b), (c), (d) represent samples from 1 to 4 respectively.

B) Scanning Electron Microscop Characterization

In addition to the DLS analysis, the SEM images are illustrating the polydispersity of samples 1 and 4. The bigger particles for sample 3 with the high degree of monodispersity are also shown clearly in the image. In addition, the image for sample 4 shows high degree of agglomerations.

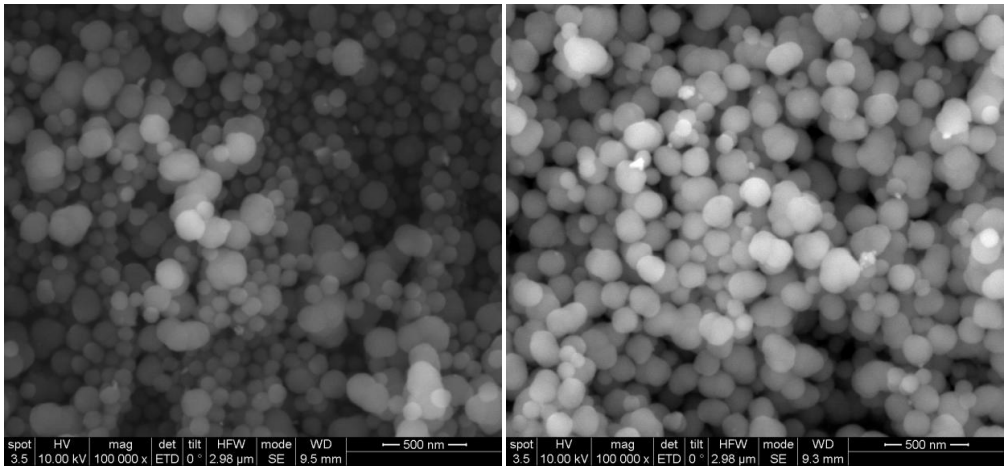

(a) (b)

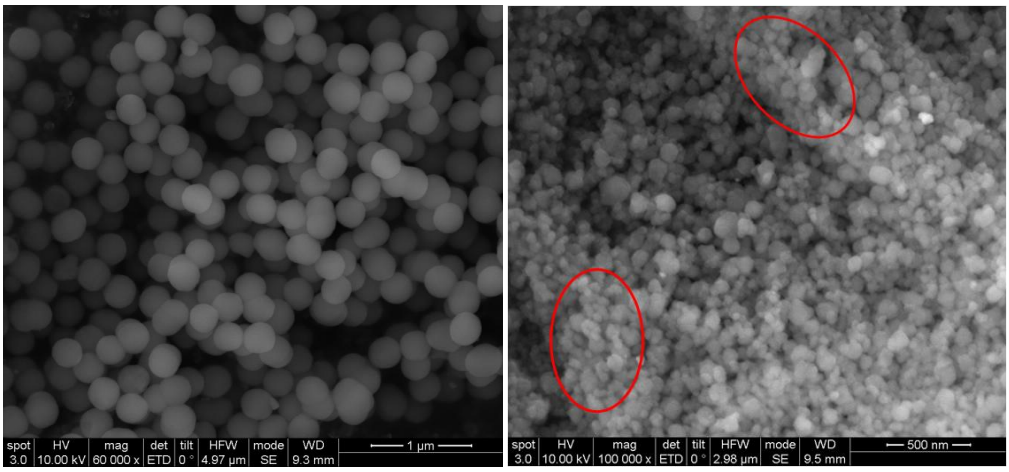

(c) (d)

Figure 16: SEM characterization for the four samples; (a), (b), (c), (d) represent samples from 1 to 4 respectively.

The size distribution of the nanoparticles was also measured using he SEM images and the National Instruments IMAQ vision builder software. Figure 17 shows the results corresponding to measuring 100 nanoparticles of batch number 3. The mean nanoparticle diameter obtained from the IMAQ was 300±20 nm and it is smaller in accordance to the DLS measurements. Because DLS is measuring the hydrodynamic diameter of the nanoparticles, the results from DLS are not the same from the IMAQ.

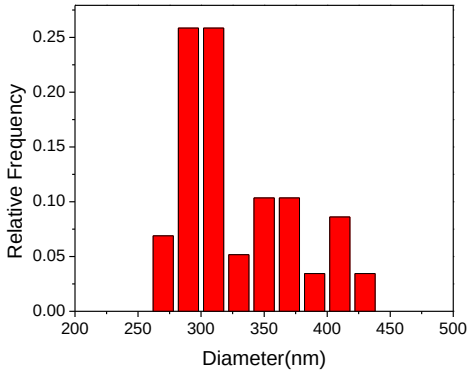

Figure 17 : Particle size distribution obtained by IMAQ for batch 3.

4.1.1.2 Conventional stirring method

A) Dynamic Light Scattering

Table 4 shows the results from synthesis of three solutions and their characterization using DLS. Evidently, the value for the polydisperse index is a clear indication of the high degree of monodispersity for the three samples. By the same way as dedicated in the table, the nanoparticles have a mean particles size in the range of 140±15 nm.

In addition, the reproducibility of the conventional stirring method in terms of the synthesis yield and the concentration of the produced silica nanoparticles had been observed. The reproducibility of this method lies in three reasons: (1) controlling the addition of the tetraethyl orthosilicate as slow as possible, (2) Fixing the stirring rate from the beginning of the process and keep it constant, (3) Controlling the temperature of the stirring plat while the whole process at 30^{o}C.

Table 4: DLS characterization for 3 batches of silica synthezed using conventional stirring method

Sample/ Data	1	2	3
Mean Diameter (nm)	155.3	143.9	139.3
Mean Diameter fitting (nm)	No fitting	No fitting	135.4
FWHM (nm)	No fitting	No fitting	53
PDI	0.031	0.022	0.03
Concentration (mg/ml)	3.48	3.22	3.25
Yield (%)	25.04	23.96	24.2
PH	8.6	8.9	8.7

As same as in the ultrasonic batches, the third batch had been fitted to observe the mean particles size diameter. The black curve and the red curve represent the DLS distribution and the fitting curve according to Gauss non-linear fitting. Figure 18 shows the DLS characterization for the three samples.

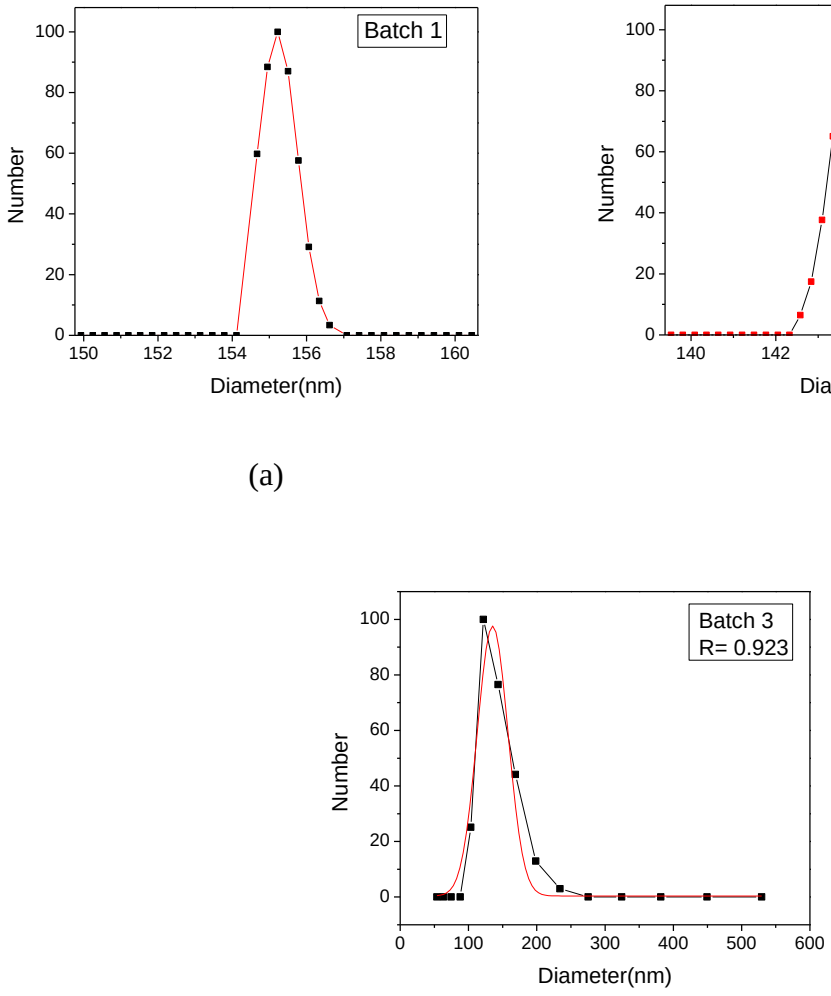

(a) (b)

(c)

Figure 18: DLS characterization for the four samples; (a), (b), (c) represent samples from 1 to 3 respectively.

B) Scanning Electron Microscop Characterization

The three samples were characterized by SEM and three of them show the same particles arrangement and morphology. Figure 19.a shows the SEM images for one sample of them. A second method was also used to confirm the size of the nanoparticles produced, the size was determined statistically using National Instruments IMAQ vision builder software as shown in figure 19.b. The mean nanoparticle diameter determined by IMAQfor measuring 100 nanoparticles was of 110±10 nm.

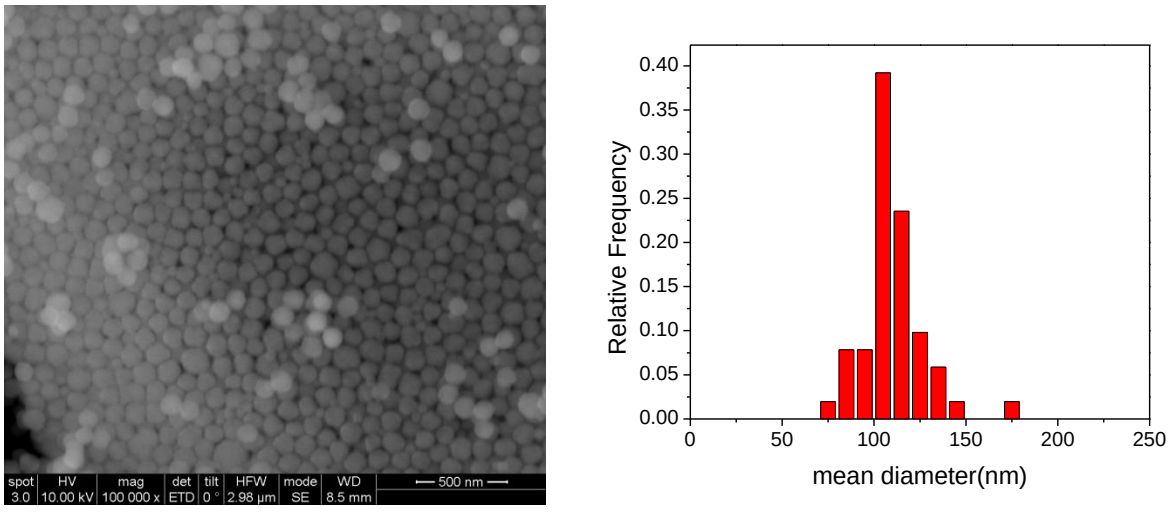

(a) (b)

Figure 19: Particle size distribution obtained by: (a) SEM , (b) IMAQ .

Figure 19 (b) shows that there were small nanoparticles in the solution, which, the DLS could not recognize them because it measures the hydrodynamic diameter.

4.1.2 Silver nanoparticles characterization

Six different batches had been prepared using the Microwave assisted polyol synthetic approach. All the batches had been characterized using the Dynamic Light Scattering and the Transmission electron microscope and Ultraviolet–visible spectroscopy.

4.1.2.1 DLS characterization

In order to estimate the nanoparticl diameter, DLS characterization had been done for the 6 different samples (figure 20).

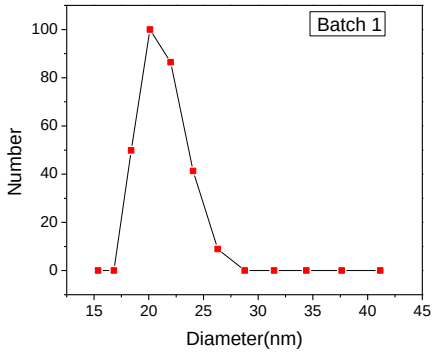

(a)

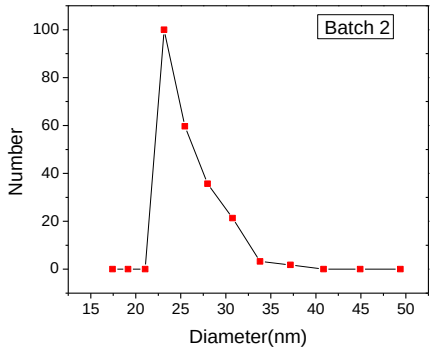

(b)

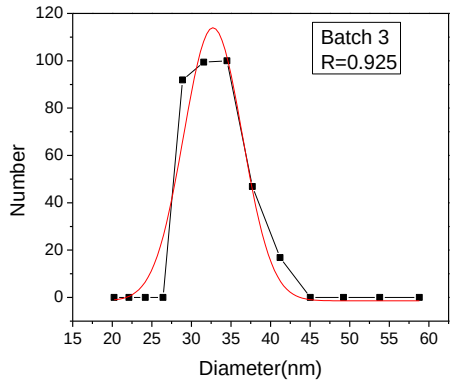

(c)

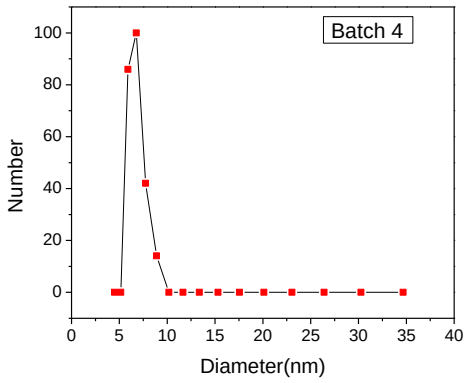

(d)

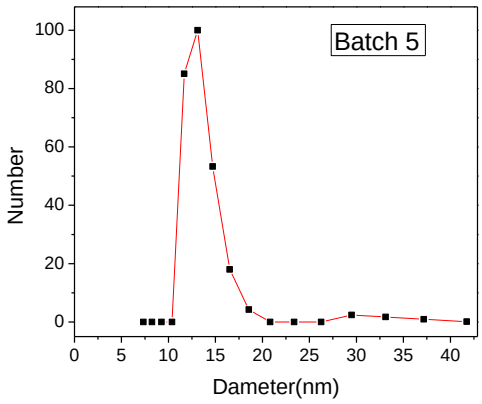

(e)

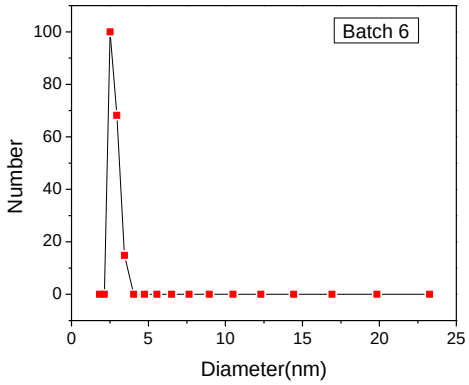

(f)

Figure 20: DLS characterization for the six samples from (a) to (f) represent samples from 1 to 6 respectively.

For batches 1, 2, 3 and 5 the nanoparticles have a particles size in the range of 10 - 30 nm .While in the batches 4 and 6 the particle size distribution is different as the particles have a diameter in the range of 2.5 - 5 nm. The third batch distribution had been fitted and according to Gauss non-linear fitting the mean diameter is around 32.7 nm and FWHM 8.77 nm. In addition, table 5 is summarizing the particle diameter, concentration, yield and the polydispearsity index for each batch. In all the batches bigger particles have been appeared in the volume distribution

Table 5: Comparison between six samples of siver nanoparticles characterization

Sample/ Data	1	2	3	4	5	6
Mean Diameter (nm)	21.2	25.6	33.1	6.8	13.7	2.7
PDI	0.063	0.094	0.218	0.298	0.305	0.321
Concentration (mg/ml)	4.26	3.28	1.7	2.05	3.1	12.54
Yield (%)	-----	------	33.35	41.51	15.3	31

The yields of the first two samples are illogical values and this could be due to an experimental measurement error specially the concentration measurement. In addition, the centrifugal temperature was 17 ^{o}C for the last three samples and we could recognize that the particles mean diameter had been decreased when the centrifugal temperature decreased. The results show different particles diameter in each sample and that could be because of the different accelerate in the addition of polyvinyl pyrrolidone "PVP" or the cooling bath temperature or the stirring speed in each sample.

4.1.2.2 Transmission Electron Microscope characterization

In order to estimate the shape, size and morphology of the synthesized nanoparticles TEM images had been taken for each sample. Figure 21 show the TEM images for the six samples. As shown in the image for batch 6, the particles diameter is smaller than the other batches particles and this result is ascertaining the results from the DLS distribution for the particles.

The bigger particles, which appeared in the DLS, have been shown also in the TEM images, but in the TEM bigger particles and aggregations have been appeared. As the inset images show the huge particles and aggregation which appeared in each sample.

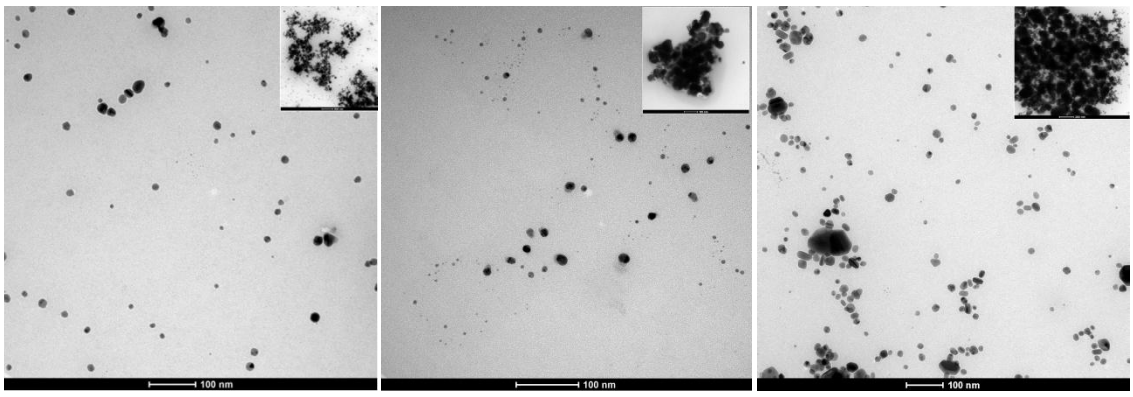

(a) (b) (c)

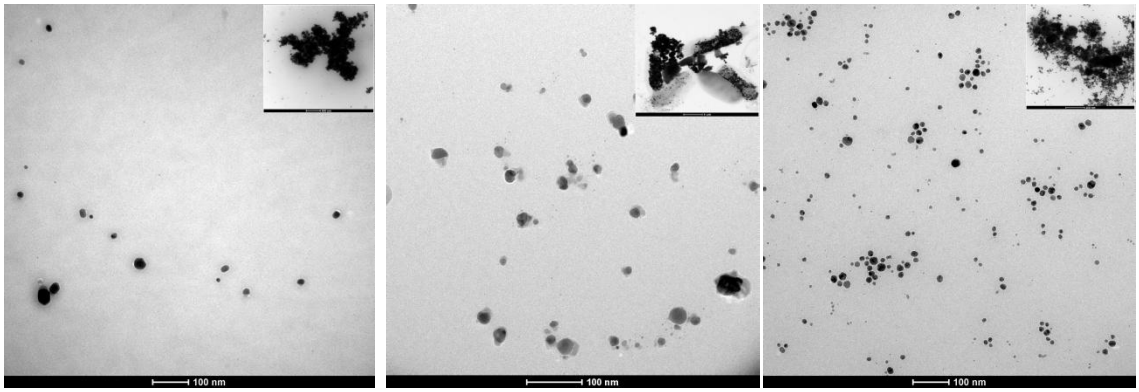

(d) (e) (f)

Figure 21: TEM characterization for the six samples; from (a) to(f) represent samples from 1 to 6 respectively.

4.1.2.3 Ultraviolet visible spectroscopy (UV-vis)

Figure 22 is showing the Ultraviolet–visible absorption peaks for the six silver nanoparticles sample synthesized in this work.

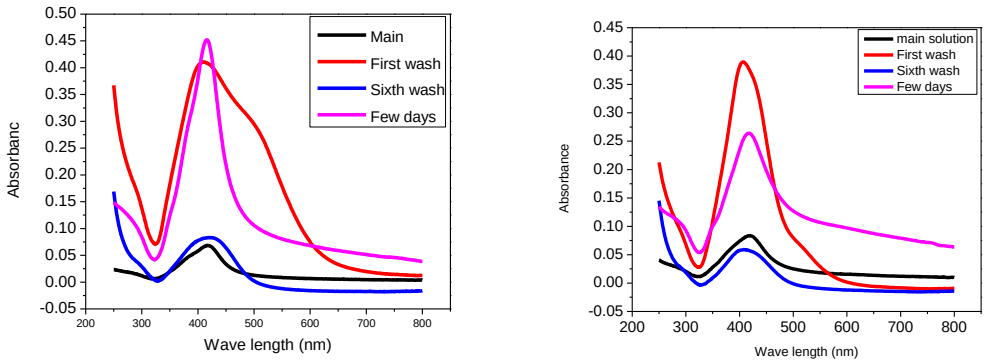

(a) (b)

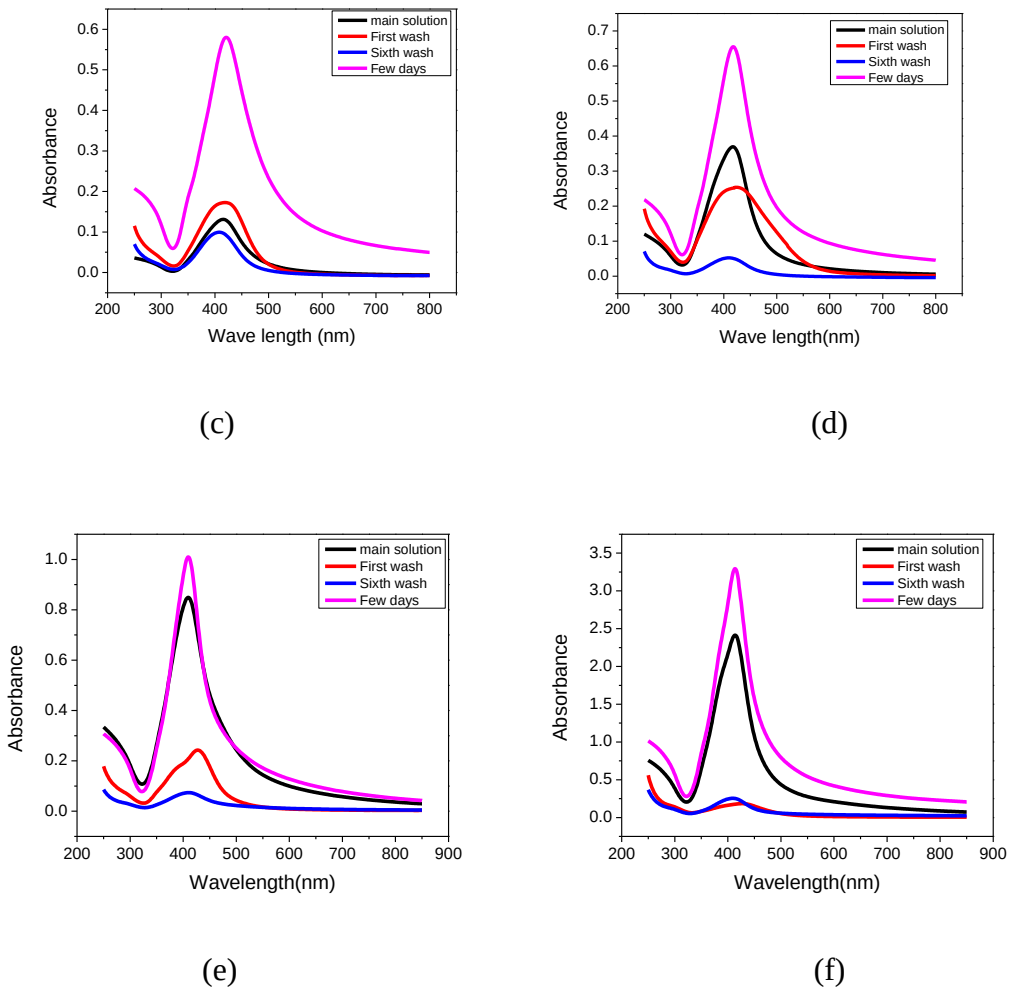

Figure 22: UV-vis characterization for the six samples; from (a) to (f) represent samples from 1 to 6 respectively.

The peak around 400 nm corresponds to the surface plasmon resonance (SPR) of the silver nanoparticles [30]. As showing in the absorption peaks for the first and sixth supernatant, the first wash supernatant was still contain silver nanoparticle and the amount decreased in the sixth wash. In addition, the effect of the time after synthesis could be observed from the difference between the black and the purple peaks, which referred to the main feed and same sample after few days and this change could be due to the sensitivity of silver nanoparticles to the light.

4.2 Fractionation and separation process

4.2.1 Silica nanoparticles solutions

The two different batches prepared by ultrasonic method, i.e. polydisperse solution and conventional stirring, i.e. monodisperse solution were filtered using a cross flow filtration method to evaluate the 60 nm membranes.

4.2.1.1 Filtration of polydisperse solutions

Due to the non-reproducibility and the different particle size in the four batches, a mixture of the four samples had been prepared and used for the filtration process. The mixture has a concentration of 10.48 mg/ml. Figure 23 shows the particle size distribution of the mixture measured using DLS. The volume distribution shows the bigger particles in the mixture that do not appeared clearly in the number distribution.

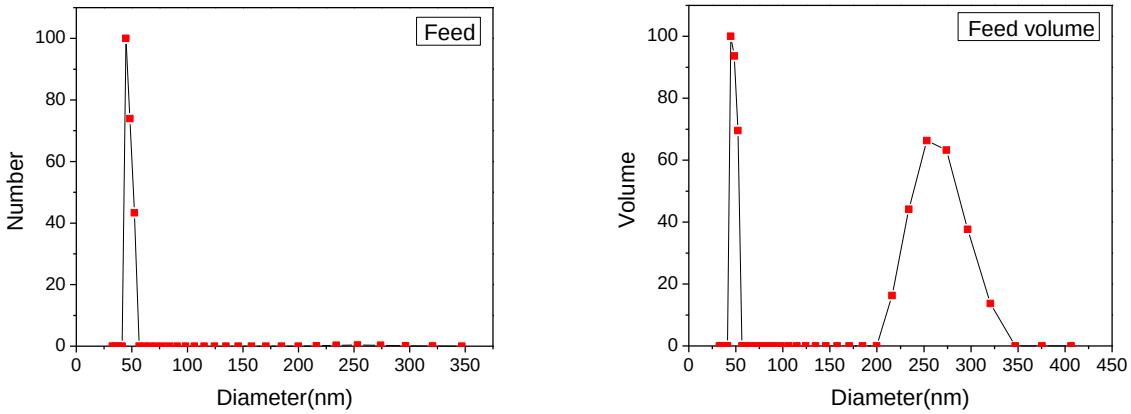

(a) (b)

Figure 23: DLS characterization of the mixed ultrasonic batches.

The results show the bimodal particle size distribution in the ranges of 40±10 nm and 250±20 nm and that explains the 0.103 polydispersity index for this mixture.

The filtration process for this solution had been done with the 60 nm alumina membrane. The cross flow filtration has been done at constant flow. The feed solution has beed prepared with a concentration of 2 mg/ ml and flow rate of 2 ml/m. The pressure was measured during the process and it was increasing from 0.025 - 0.955 MPa, see figure 24, after 23 minutes the pressure was stable at 0.945 MPa.

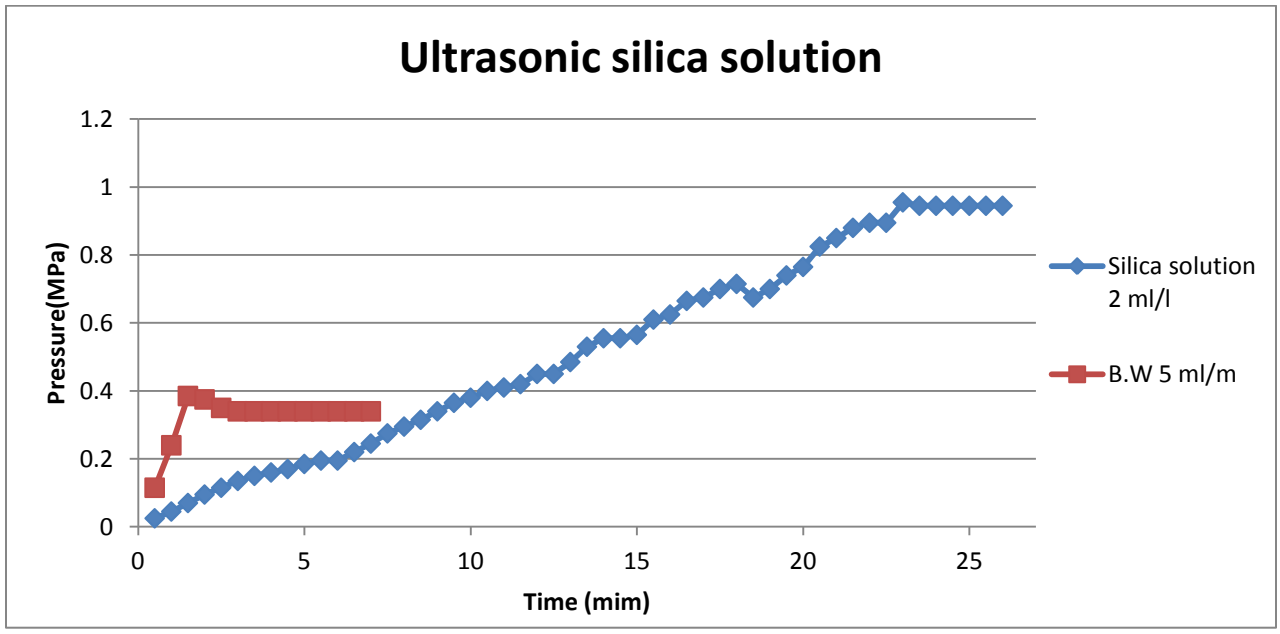

Figure 24: Pressure vs. time during the cross-flow separation process for the ultrasonic silica mixture solution.

The permeate solution color was pale milky while the retentate was dark milky solution. The permeate and retentate solutions had been characterized by DLS. Figure 25 show the particles size distributions in both solutions after filtrations.

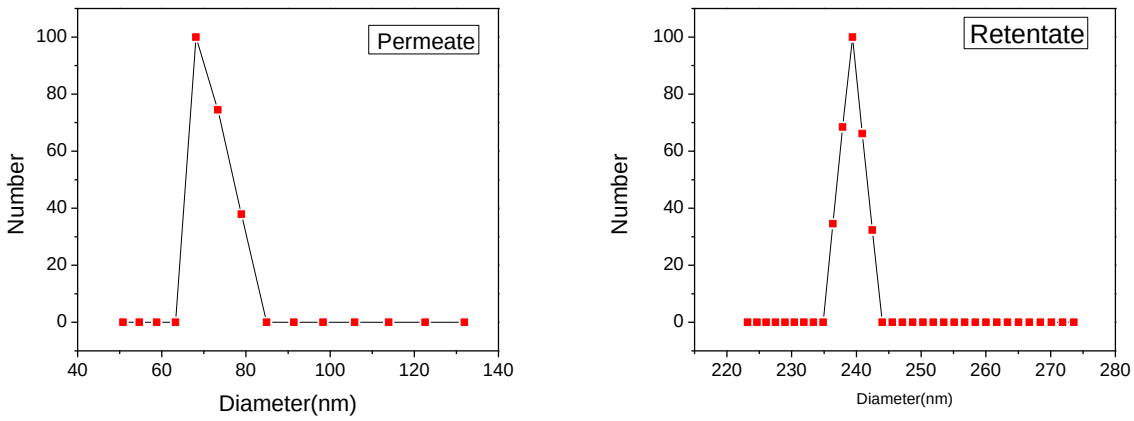

(a) (b)

Figure 25: DLS characterization for (a) permeate, (b) retentate solutions of filtration the polydispere silica solutions.

The results show the permeate solution has almost all the particles which have diameter smaller than or equal to the membrane pore sizes. The bigger particles have been collected in the retentate solution.

The mean particle diameter in the permeate solution was around 73±5 nm while it was of 239±0.4 nm in the retentate solution. For the retentate the polydispersity index was 0.085 which explain the narrow peak in the size distribution. While it was 0.134 in case of the permeate solution because it is containing a boarder particle size distribution (figure 25 a).

In order to recover the silica nanoparticles from the filtrate cake formed on the surface of the membrane a backwash process was done. In order to achieve a strong and high pushing for the nanoparticles, the process was done at flow rate of 5 ml/m. The pressure was fluctuating in the range 0.115 - 0.385 MPa. The pressure starts rising until it reaches a maximum value at 0.385 MPa and then decreased and started to be constant at 0.34 MPa (see figure 24). Figure 25 shows the particles size distribution for the collected backwash solution after 3 minutes.

The results from DLS show that the solution has a polydispersity index of 0.124 and mean particle diameter 238.5±0.1 nm.

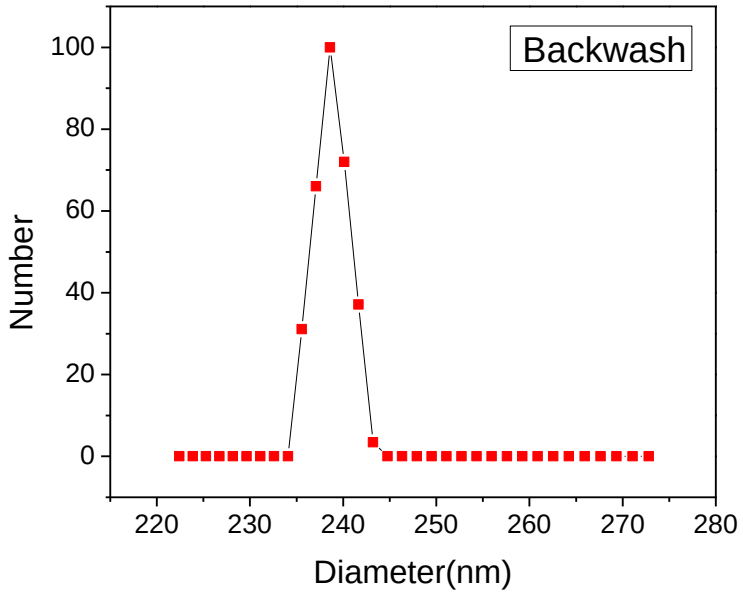

Figure 26: DLS characterization for the backwash solution for the polydispersity silica solution.

According to the previous filtration process results, the fractionation process was successful for the polydisperse silica nanoparticles solution by having a smaller particles in the range of 73±5 nm in the permeate side while the bigger particles in the range of 239±0.4 nm were collected in the retentate side. Additionally, the concentration of permeate solution has measured and it was 0.34 mg/ml. Thereafter the % of rejection[26] had calculated resulting in 83 % of the polysiperse silica solution had been rejected using the 60 nm membrane.

4.2.1.2 Monodisperse silica solution

A mixture solution had been prepared from the initial samples. The mixture particles size distributions were measured by using DLS. Figure 27 shows the number and volume distribution for the mixture solution.

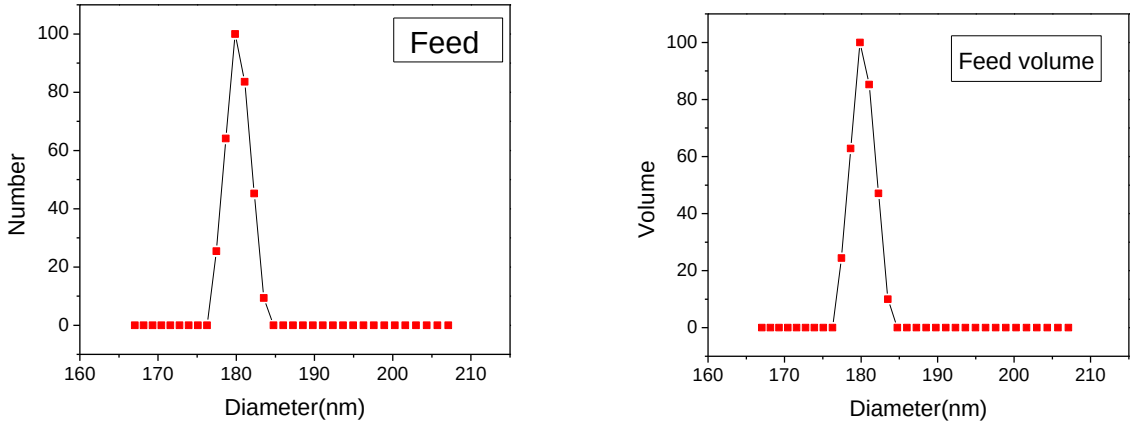

(a) (b)

Figure 27: DLS characterization for the conventional stirring batches mixture.

The results from DLS distinct the mean particles diameter for the mixture is 180±0.2 nm. The polydispersity index for this mixture was 0.083, which depict the similarity between the number and the volume distribution.

The feed mixture was prepared with a concentration of 2 mg/ml then the mixture had been fractionated using the 60 nm pores membrane. The fractionation had been done by operating cross flow, constant flow process. The cross flow process had been done at 2 ml /m flow for feed solution.

The pressure was fluctuating during the process between 0.025 - 1.005 MPa. The process was perpetuated until the pressure started to be constant and reach a plateau. The maximum pressure was 1.005 MPa during the 10 minutes of filtration process but it started to be constant after 8 minutes at value of 0.885 MPa. Figure 28 is showing the fluctuation of the pressure during the filtration process versus time.

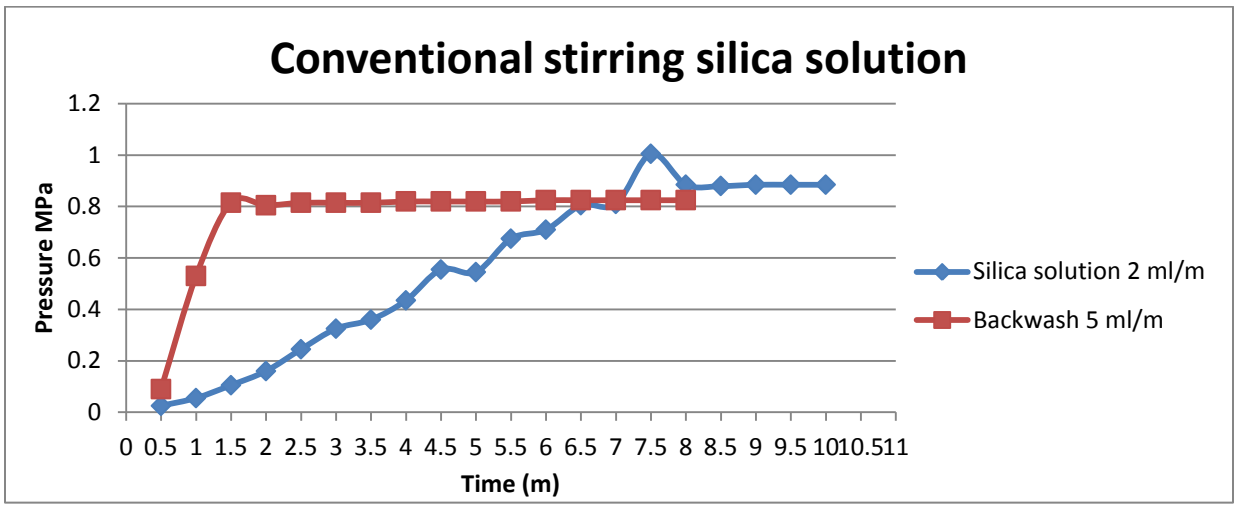

Figure 28: Pressure vs. time during the cross-flow separation process for the conventional stirring silica mixture solution.

Although, the permeate solution was almost clear colorless solution while the retentate was dark milky solution. The particles in the permeate solution were having diameters in the range of 76.3±0.09 nm. The permeate solution concentration was measures in order to estimate the % of rejection[26]. The measurement shows that the permeate has a concentration of 0.86 mg/ml. Thereafter the % rejection was 57%.

This result means that either there were smaller particles in the feed solution were successful to path through the 60 nm pore size membrane or these smaller particle could be due to fragmentation of the nanoparticles according to the pressure which was applied during of the process. Figure 29 is showing the size distribution of the particles in both permeate and retentate solutions.

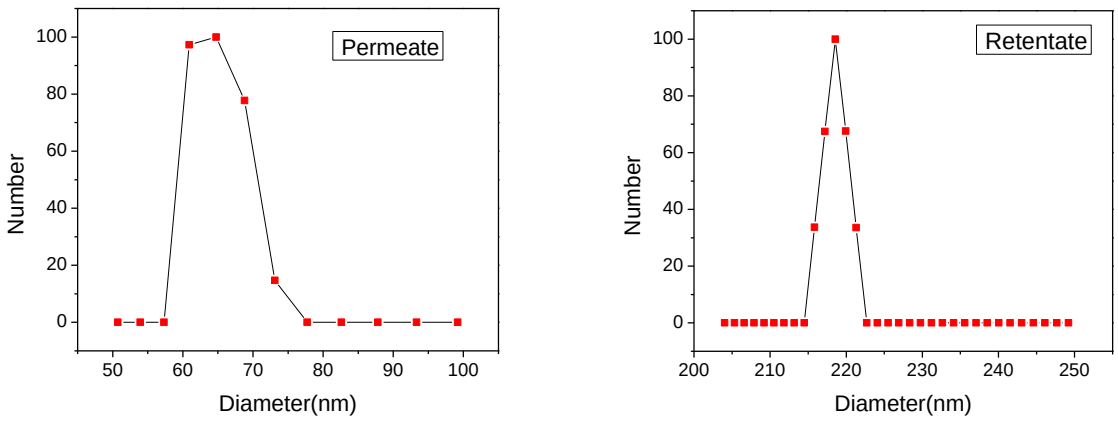

(a) (b)

Figure 29: DLS characterization for (a) permeate, (b) retentate solutions.

In order to estimate the particle size for the nanoparticles, which were in the filtration cake on the membrane surface, a backwash process was done. The backwash process has been done at constant higher flow than the cross flow process in order to achieve the strong and high pushing for the nanoparticles.

The pressure during the backwash process was plotted versus the time. Figure 28 shows that the pressure in the backwash process was fluctuating between 0.05 - 0.825 MPa and the process was lasted for 8 minutes but the process engrossed around 5 minutes to reach a fixed pressure at 0.825 MPa.

Similarly to the previous results , the backwash pressure profile indicate that after a sharp increase the membrane is clean.

The particle size distribution was measured by using DLS in order to estimate the mean Particles size of the backwash solution, figure 30 show the DLS graph. The mean diameter for the particles was of 194±0.38 nm.

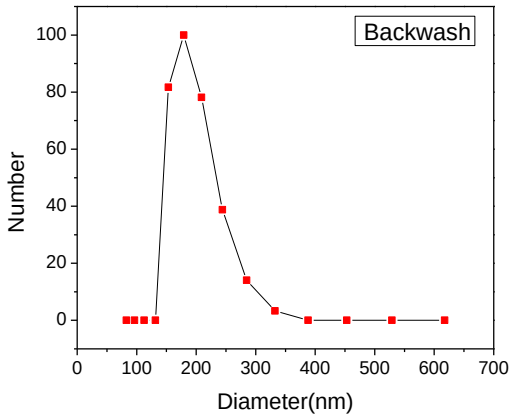

Figure 30: DLS characterization for the backwash solution.

Table 6 shows a summary for filtration process for both the ultrasonic and the conventional stirring processes in terms of polydispersity index, concentration and rejection.

Table 6: Summary of silica nanoparticles fractionation.

Method /Data	Polydisperse solution				Monodisperse solution			
	Feed	***Permeate***	***Retentate***	***Backwash***	***Feed***	***Permeate***	***Retentate***	***Backwash***
Particle mean diameter (nm)	40±10 &250±20	73±5	239±0.4	238±0.1	180±0.2	76.3±0.09	218±0.6	194±0.038
PDI	0.085	0.134	0.085	0.124	0.085	0.139	0.073	0.08
Rejection %	83%				53%			

In Wang et al [17] work, the % rejection for the monodisperse silica nanoparticles solution filtrated by dead end was given of ≥ 99%, but they only eliminate the silica nanoparticles having diameters ≤ the pores of their membrane CNF-98. While based on the stated results in this thesis a fractionation process was successful to reject 83 % of polydispere and 53% of monodisperse silica nanoparticles, producing monodiperse solution of the smaller particles in the permeate.

4.2.2 Separation and filtration of silver nanoparticles

According to the different particles diameter, concentrations, polydiepersity and the yield of the produced silver nanoparticles batches. Two different mixtures of the silver nanoparticles had been used. The filtration of the silver nanoparticles had been done by using the 5 nm pores membrane due to the smaller nanoparticles that the silver has compared to the silica nanoparticles. Additionally, the silver solution had been filtrated with two different filtration procedures. Dead-end procedure was used for the low concentrations and cross-flow for the higher concentrations.

4.2.2.1 Dead-end procedure

Three different concentration solutions (0.01, 0.1 and 0.25 mg/ml) had been prepared to be tested with dead-end filtration using three different 5 nm membrane. The filtration processes were done at constant flow 2 ml/m for the feed solution. The mixture feed solution (S1) particles size had been characterized by using DLS. Figure 31 shows the particle size distribution for both number andvolume. The volume distribution is in order to obtain the bigger particle.

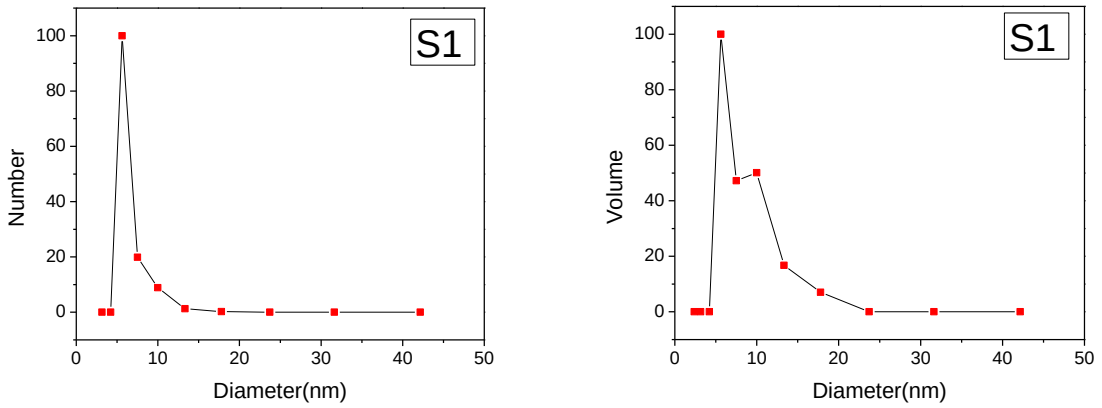

(a) (b)

Figure 31: DLS characterization for mixed silver nanoparticles solution (S1) ;(a) Number and (b) Volume distribution.

A) Feed with 0.01 mg/ml

A feed solution of concentration 0.01 mg/ml was filtrated using 5 nm membrane. The filtrate solution was totally clear and colorless. Figure 32 (a) shows the solutions before and after filtration. The filtrate concentration was very low, so it was not possible to measure the size distribution for the nanoparticles using the DLS. Alternatively, the filtrate nanoparticles were characterized by TEM and UV-vis respectively. Although, the TEM images did not show the nanoparticles size also due to the diluted solution as it shown in figure 32 (b) and the UV-vis spectra shows almost 100 % rejection figure 33(b). The solution had been concentrated by evaporating the water from the solution in order to estimate the particle size distribution and measure the exact concentration and rejection % of the filtrate solution. The evaporation process was at 60^{o}C and lasted for 4 hr in which, initial volume for the filtrate was 22.8 ml and became 2.5 ml after evaporation. The solution after evaporation had a concentration of 0.0021 mg/ml (2.1 ppm) measured by MCP-AES. A rejection percentage of 88% was calculated based on the concentration value. Although, it was not possible again to measure the nanparticles size distribution by using the DLS analysis but the TEM for the filtrate after evaporation could show the nanoparticle of size 6±2.5 nm. Figure 32 (c) shows the TEM image for the filtration solution after evaporation.

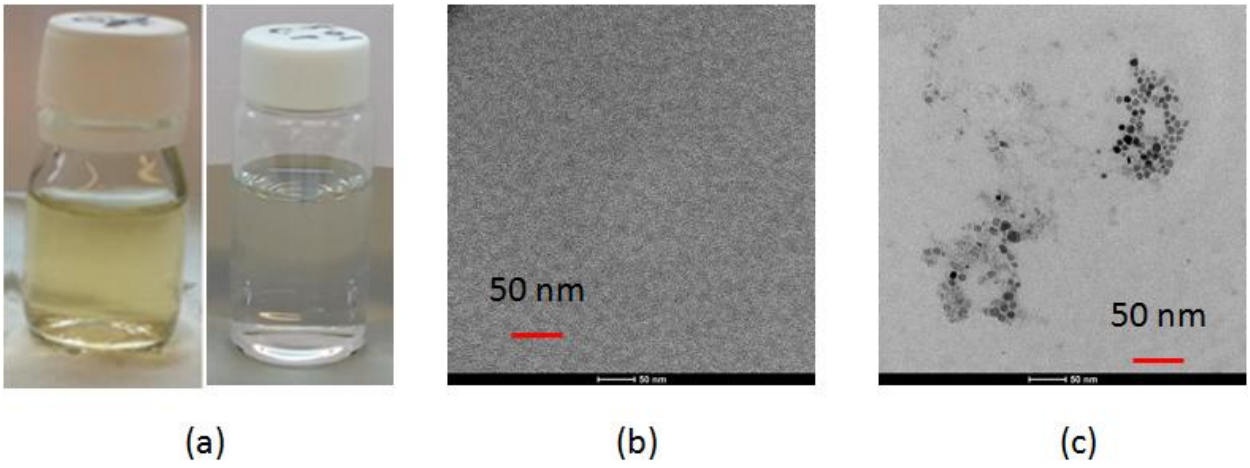

Figure 32: Filtration process for 0.01 mg/ml feed ; (a) solution before and after filtration , (b) TEM image for filtrate , and (c) TEM image for filtrate after evaporating the water .

Therefore, the UV-vis spectroscopy alone or the TEM images for high diluted solution are not good techniques for characterize the silver nanoparticles after a filtration process. Consequently, the rejection percentage of 100 % which, estimated in Wang et al. work[17] or the 20 % estimated by Mekawy et al. [18] are not accourt as it had been calculated based on the Uv-vis spectra only. Despite this, comparing the rejection % obtained in this work with published work, the 88 % rejection obtained for the silver nanoparticles solution in the range of 5-20 nm at variance to the monodisperse solution of a particle diameter of 25 nm in Wang et. al[17].

In order to estimate the nanoparticles size IMAQ software was used to count the nanoparticles, figure 33 (a) is showing the particle size distribution of 100 nanoparticles obtained by IMAQ. Thereafter, in order to recover the nanoparticles, which were blocked in the membranes pore a back flush process had been done. The flow (2 ml/m) for the back flush was not enough to push the nanoparticles from the pores and the resulted solution was clear. Additionally, the absorption spectra of the feed, the filtrate before and after the evaporation and the backwash solution have been measured using UV-vis and are shown in figure 33 (b).

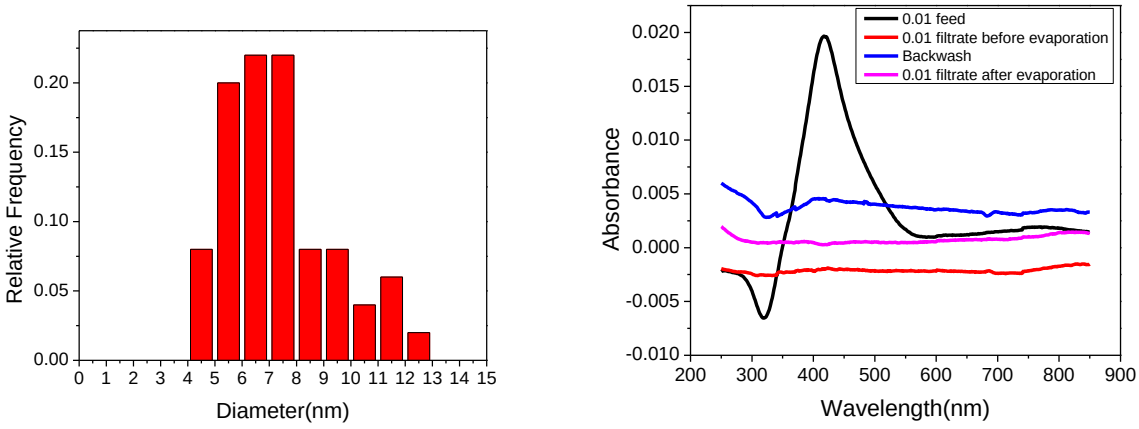

(a) (b)

Figure 33: (a) Particle size distribution obtained by IMAQ, and (b) UV-vis spectra for feed, filtrate before and after evaporation and backwash solutions.

From the figure, the nanoparticles have diameters in the range of 4 - 13 nm. The higher portion of the nanoparticles was in the range of 5 - 8 nm these nanoparticles, which are bigger than the 5 nm pores of the membrane could be formed during the evaporation process. On the other hand, the curve for the filtrate after evaporation has higher absorbance than before as it shown in figure 33 (b) the red and purple curves.

B) Feed with 0.1 mg/ml

A feed solution of concentration 0.1 mg/ml was filtrated using 5 nm membrane. The filtrate solution was light yellow. Thereafter, a backwash process had been done in order to recover the nanoparticles, which were crammed inside the 5 nm pores of the membrane. The flow for the backwash process was 5 ml/m in order to be higher than the feed flow. Figure 34 shows the pressure versus time graph for the backwash process and for the filtration process.

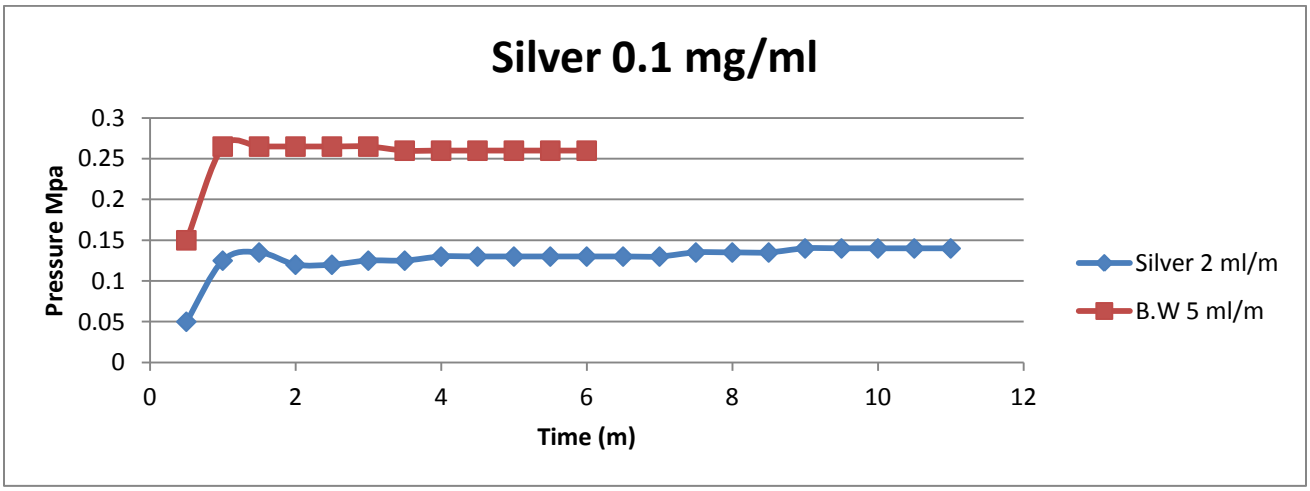

Figure 34: Pressure vs. time during the dead - end process for the 0.1 silver solutions.

The figure shows that the pressure for the backwash process is higher than the filtrate process and this is due to the nanoparticles, which were stuck in the membrane pores. The filtrate process lasted for 11 minutes until reaching a fixed pressure while it took only 6 minutes for the backwsh. The pressure for the filtrate process reached a plateau at 0.13 MPa while for the backwash process it was 0.26 MPa.

The filtrate and backwash size distribution for the nanoparticles was measured using the DLS. Figure 35 (a) shows the filtrate and the backwash solutions, (b) and (c) shows the size distribution and TEM image for the permeate solution, (d) shows the size distribution for backwash and (e) shows the UV-vis spectra for feed, filtrate and backwash solutions respectively.

(a)

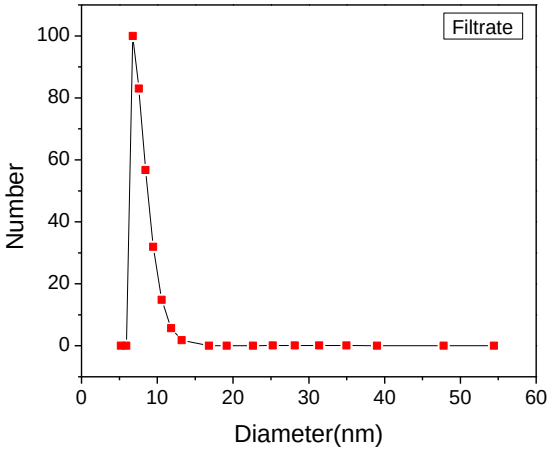

(b)

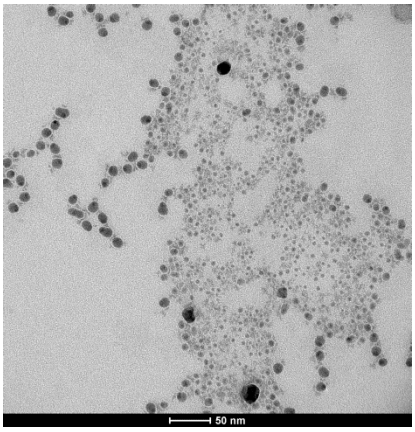

(c)

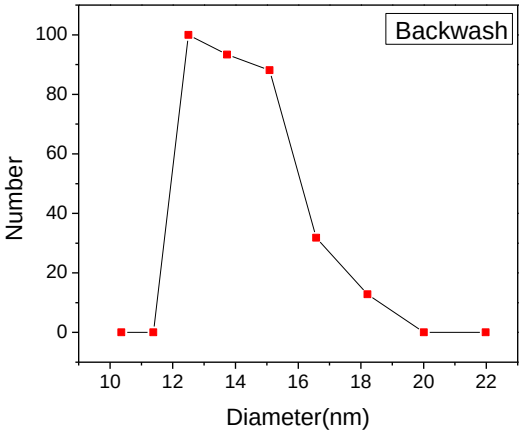

(d)

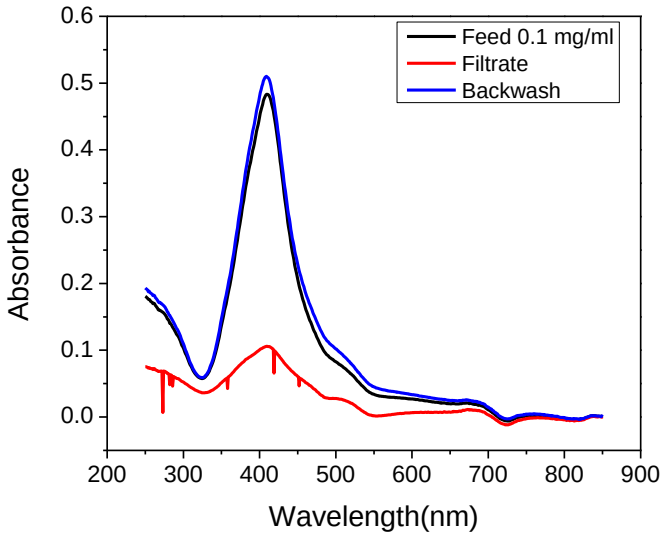

(e)

Figure 35: 0.1 Filtration process; (a) filtrate and backwash solutions, (b) and (c) DLS characterization and TEM image for the filtrate (d) DLS characterization for the backwash and (e) UV-vis spectra for feed, filtrate and backwash solutions respectively.

As shown in figure 35 (b), (c), the mean particles diameter in the filtrate solution was 7.5±2 nm and while it was 14±4 nm in the back wash solution.

C) Feed with 0.25 mg/ml

A feed solution of concentration 0.25 mg/ml was filtrated using 5 nm membrane. The filtration process was done at constant flow 2 ml/m and the produces filtrate solution was pale brown-red solution. The backwash process had been done at constant flow 5 ml/m in order to recover the nanoparticles from the membrane pores. The pressure was fluctuating during both processes and it became a place of interest. Figure 36 is showing the pressure versus time graph for both filtration and backwash process.

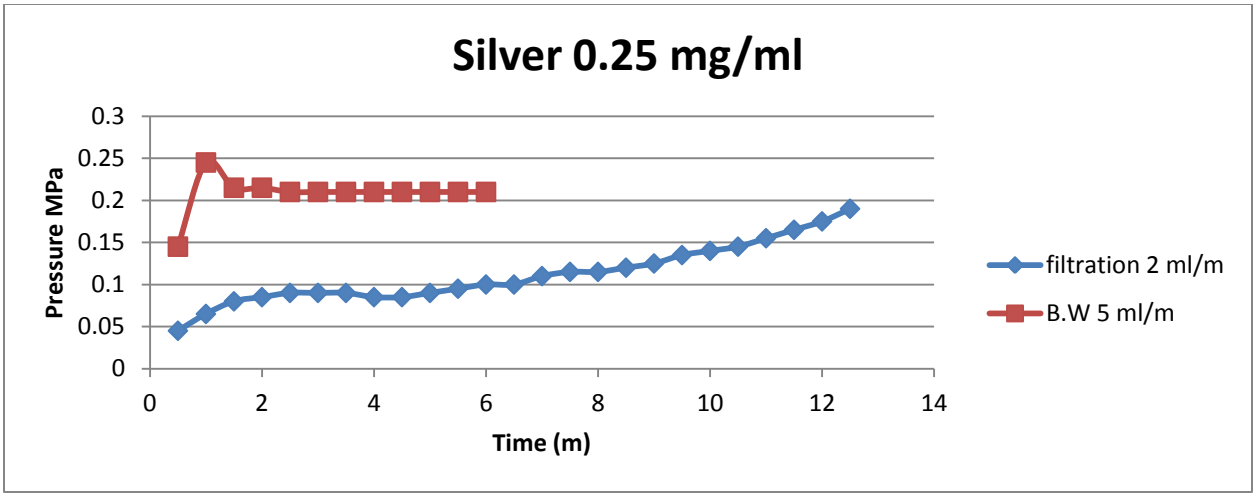

Figure 36: Pressure vs. time during the dead - end process for the 025 silver solutions.

As it was expected, the pressure achieved filtrating the 0.25 mg/ml solution was higher, 0.19 MPa, compared to the 0.1 mg/ml solution,0.14MPa. While the backwash inversely for the 0.1 mg/ml acheived the higher pressure. Additionally, the 0.25 mg/ml solution did not reach a plateau even in more time and the backwash process reach a constant pressure value in less time compared to the 0.1 mg/ml solution.

The filtrate and the backwash solution particle diameter had been characterized by DLS. In addition, optical images were taken for both the filtrate and backwash solution. Figure 37 (a) shows the filtrate and the backwash solutions, (b) and (c) shows the size distribution and TEM image for the permeate solution, (d) shows the size distribution for backwash and (e) shows the UV-vis spectra for feed, filtrate and backwash solutions respectively.

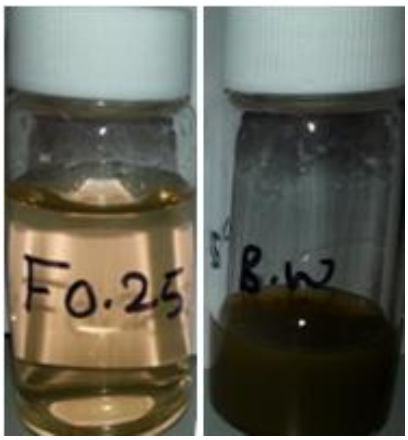

(a)

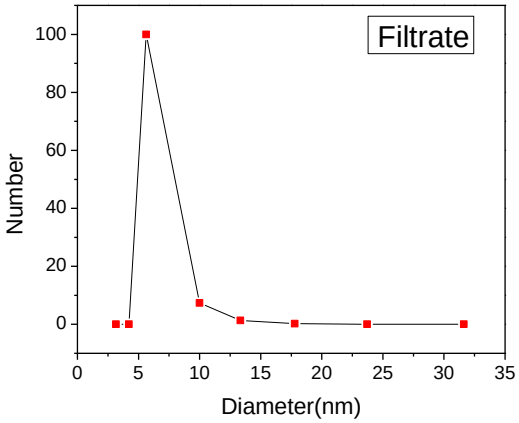

(b)

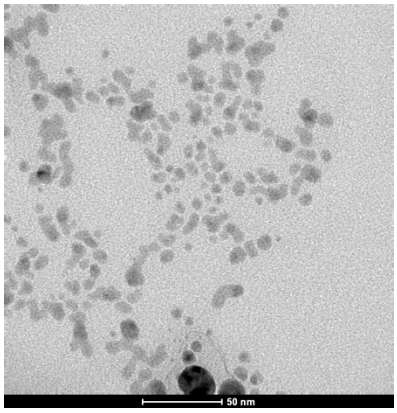

(c)

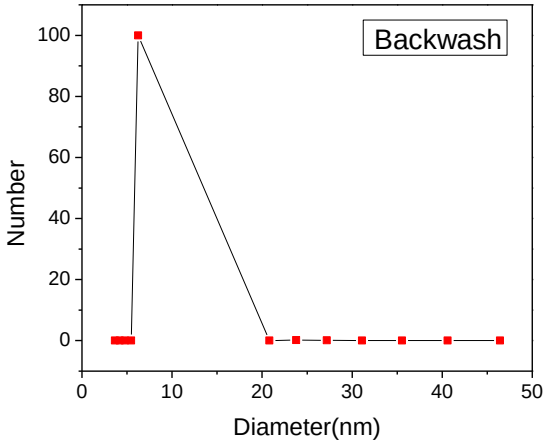

(d)

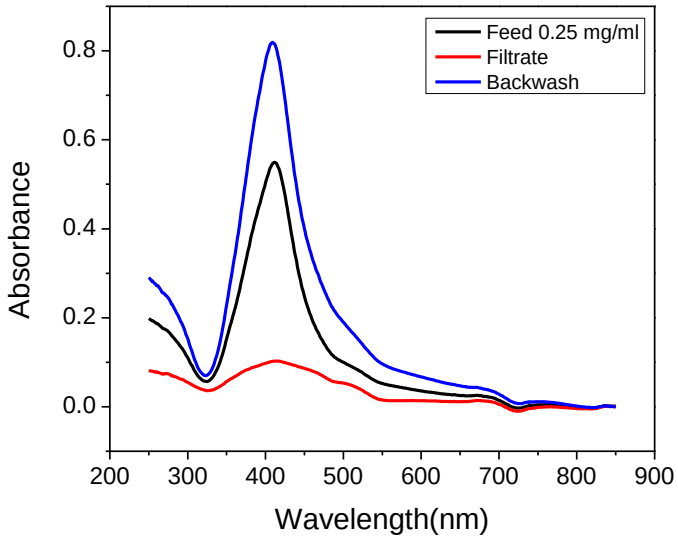

(e)

Figure 37: 0.25 Filtration process; (a) filtrate and backwash solutions, (b) and (c) DLS characterization and TEM image for the filtrate (d) DLS characterization for the backwash and (e) UV-vis spectra for feed, filtrate and backwash solutions respectively.

The DLS results show that the nanoparticles in the filtrate solution had a mean particle diameter of 6.3±0.8 nm. While for the backwash, nanoparticles had a mean diameter is 10.4±1.9 nm. Table 7, is summarizing the results from the dead - end procedure in terms of particles diameter and polydespirsty index.

Table 7: Summary of dead - end filtration.

Data/ Solution	Feed	0.01 mg/ml		0.1 mg/ml		0.25 mg/ml	
		Filtrate	Backwash	Filtrate	Backwash	Filtrate	Backwash
Mean particle diameter (nm)	6.4±0.9	6±2.5	Clear and so diluted solution	7.5±2	14±4	6.3±0.8	10.4±1.9
PDI	0.21	-----		0.053	0.05	0.07	0.288

4.2.2.2 Cross - flow procedure

Two different concentration solutions (0.5 and 1 mg/ml) had been prepared to be tested with cross - flow filtration using two different 5 nm membrane. Estimation of the amount of silver that, converted from the feed solution to ever the permeate or the retentae or the backwash attracted the attention in this project. Therefore, mass balance calculations had been done for the feed solutions.

The filtration processes were done at constant flow 5 ml/m with different membranes. The mixture feed solution (S2) particles size had been characterized by using DLS. Figure 38 is showing the particle size distribution for both volume and number distribution. The particle size of the feed was in the range of 5-51 nm. The polydispersity index of 0.306 and that illustrate why the volume distribution shows a wide range of nanoparticles.

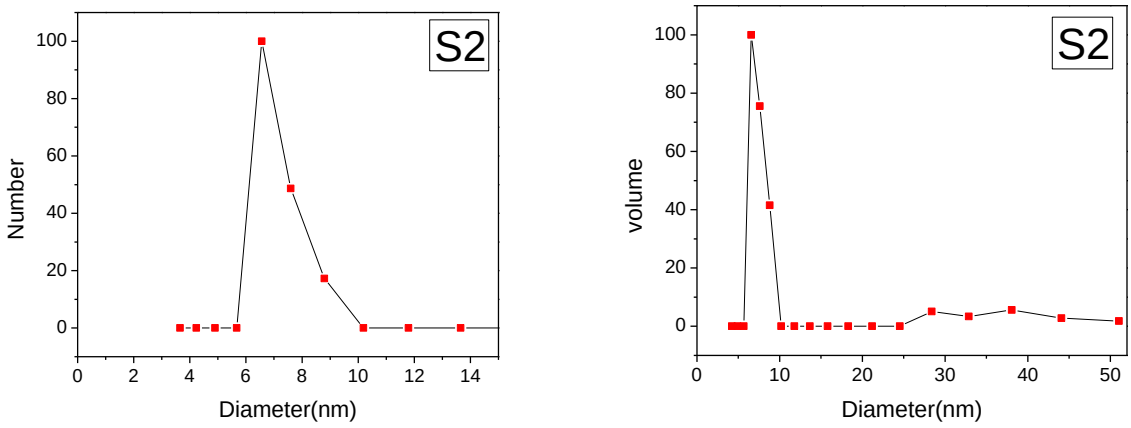

(a) (b)

Figure 38: DLS characterization for mixed silver nanoparticles solution (S2) ;(a) Number and (b) Volume distribution.

A) Feed with 0.5 mg/ml

A feed solution of 0.5 mg/ml had been introduced with a constant- flow 5 ml/m to 5 nm membrane to be filtrated using the cross- flow filtration procedure.

The filtration process was lasted for 11 minutes and the backwash for 6 minutes. Thereafter, the backwash process had been done at 2 ml/m constant flow. The permeate, retentate and backwash nanoparticles diameter were characterized by DLS. Figure 39 (a), (b) and (c) is showing the DLS distribution for permeate, retentate and backwash respectively. In addition, figure 39 (d) is showing the absorbance spectra for the filtration process solutions.

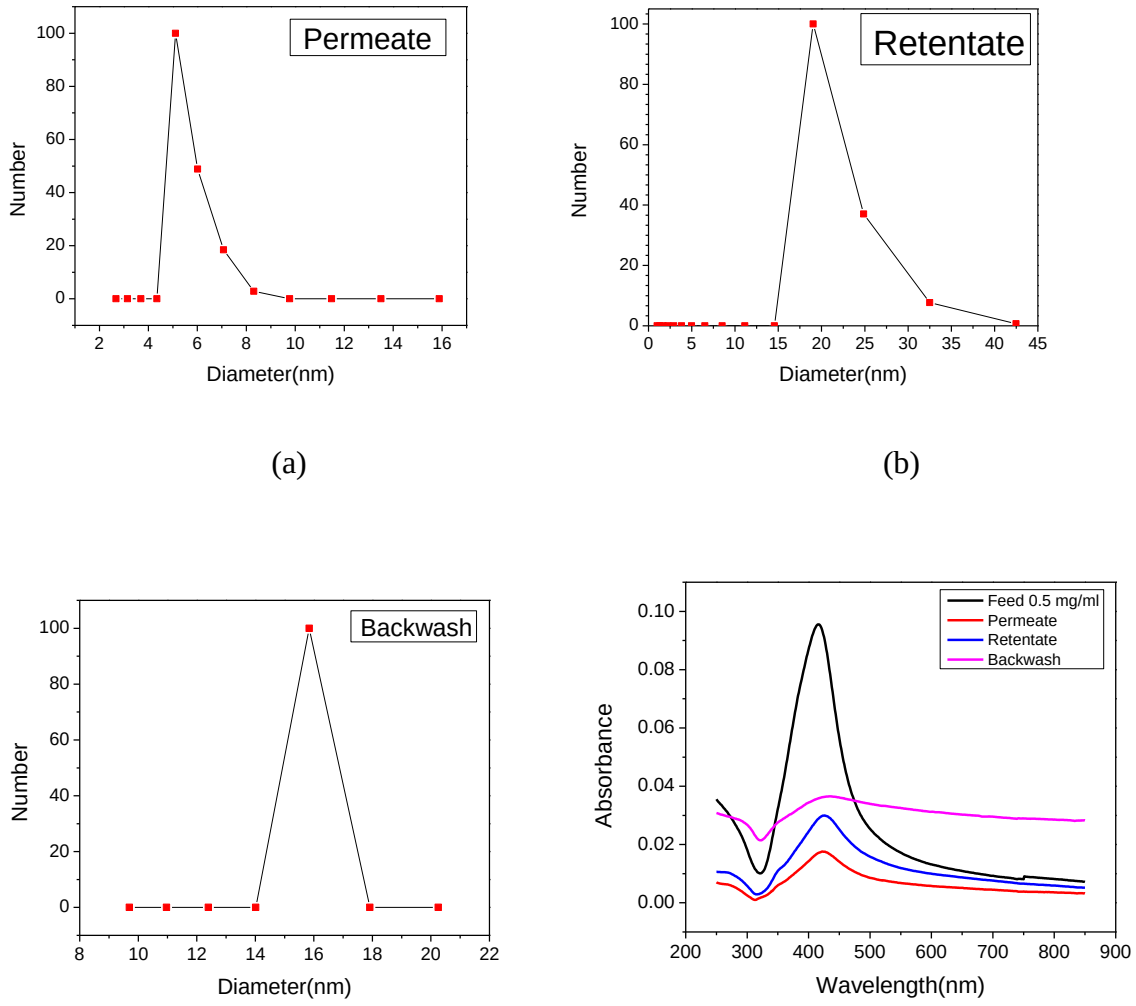

Figure 39: 0.5 mg/ml Filtration process; (a) (b) and (c) DLS characterization for filtrate retentate and backwash and (d) UV-vis spectra for feed, filtrate and backwash solutions respectively.

The results from DLS show that, the permeate solution has nanoparticles in the range of 5- 8 nm and the mean diameter is 5.5±0.5 nm. While for the retentate the nanoparticles were in the range of 19-32 nm and the mean diameter is 21.4±0.05 nm. Figure 40 shows TEM image for the permeate solution.

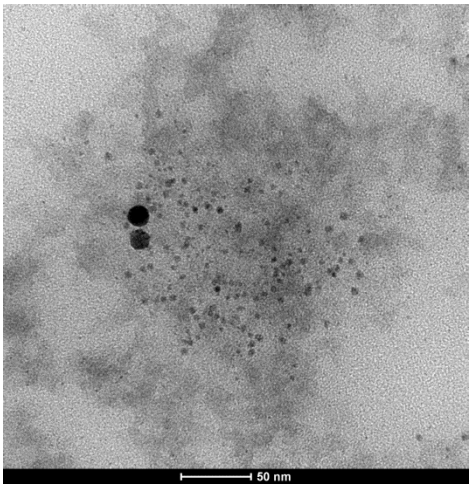

Figure 40: TEM characterization for the permeate solution.

B) Feed with 1 mg/ml

A filtration process for a 1 mg/ml solution had been done at constant flow rate of 5 ml/m, the process had lasted for 9 min. The permeate and the retentate solutions were collected in order to estimate the size distribution of both of them. Additionally, a backwash process had been done in order to recover the nanoparticles which were stuck in the membrane pores. The backwash process had been done at same conditions of the filtrate process.

The size particles distribution of the solutions had been measured using DLS. Additionally, the absorbance spectra of the feed, permeate, retentate and the backwash solution was analyzed using UV-vis spectroscopy. Figure 41, is showing the DLS characterization for all the solutions.

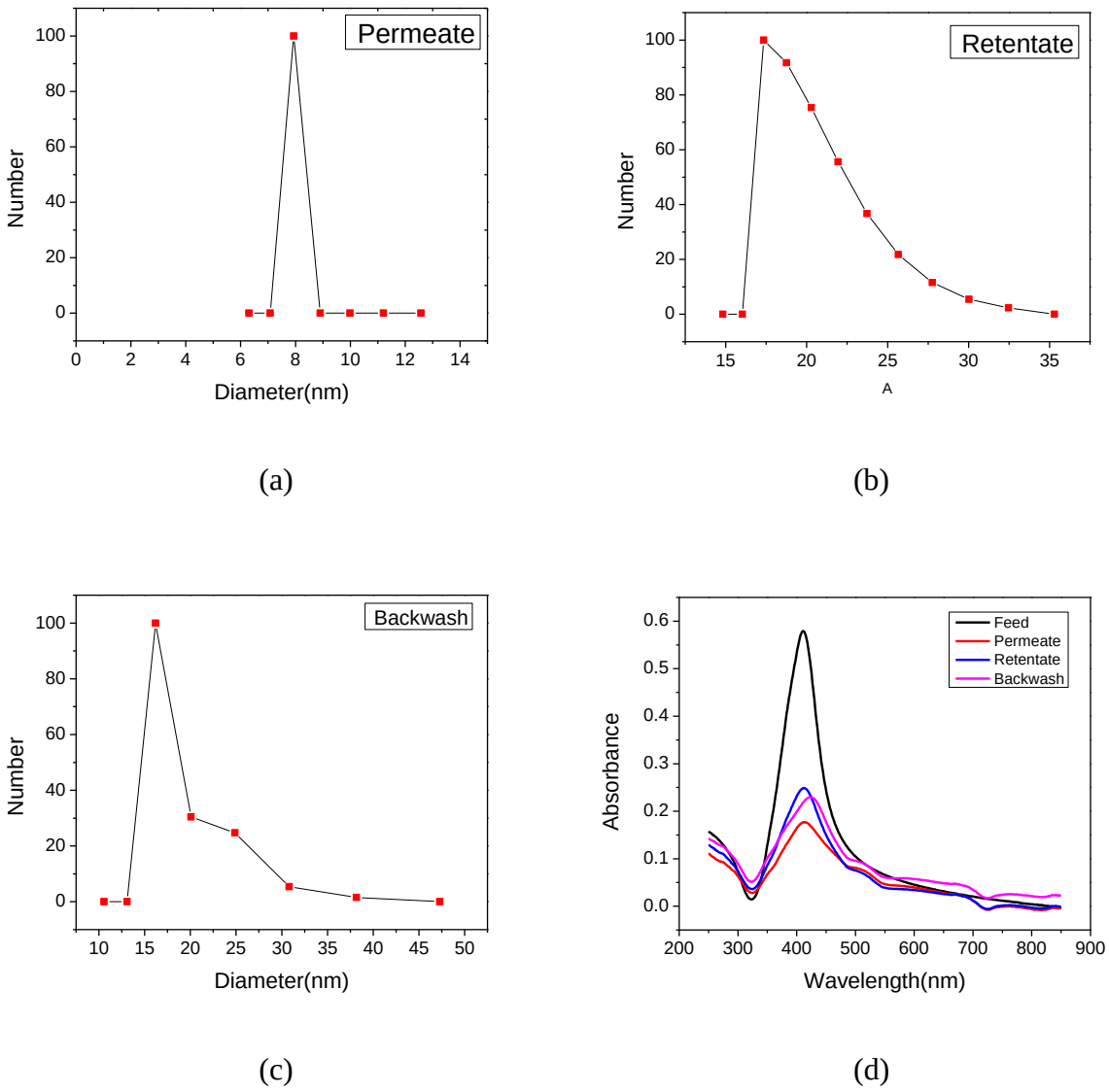

Figure 41: 1 mg/ml Filtration process; (a) (b) and (c) DLS characterization for filtrate retentate and backwash and (d) UV-vis spectra for feed, filtrate and backwash solutions respectively.

The results from DLS are showing that, the permeate solution has mean diameter of 8.7±0.123 nm while the retentate nanoparticles having mean particle diameter of 21.4±0.05 nm. On the other hand, the backwash nanoparticles were has mean diameter of of 16±0.06 nm. The

permeate solution was additionally characterized using TEM, Figure 42, is showing TEM image for the permeate solution.

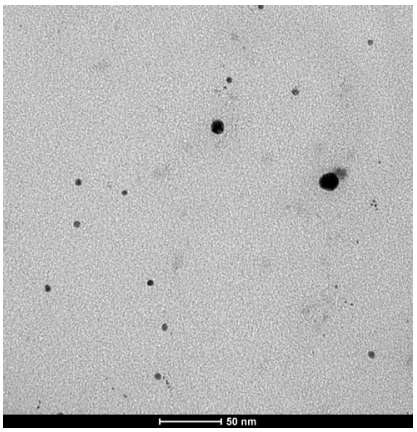

Figure 42: TEM characterization for the permeate solution.

Table 8 is the summary of the cross flow filtration in terms of the particle size and the polydispersity index in addition to the amount of silver in each stream and the mass balance percentage.

Table 8: Summary of the cross flow filtration process.

Data/ sample	0.5 mg/ml				1 mg/ml			
	Feed	Permeate	Retentate	Backwash	Feed	Permeate	Retentate	Backwash
Particles diameter rage(nm)	5-51	5-8	19-32	15.8	5-51	7.9	14-32	16-38
PDI	0.306	0.029	0.246	0.217	0.306	0.271	0.255	0.272
Amount of silver (mg)	27.5	1.35	16.24	0.702	45	23.32	15.75	5.76
Mass balance (%)	66.5%				99.6%			
Rejection(%)	95%				48.2%			

According to the result from the filtration of the 1 mg/ml silver solution, almost all the silver nanoparticles had been collected. Therefore, the membrane became a place of interest in order to explore whether there are silver nanoparticles inside the pores of the membrane or not. In order to achieve that, the membrane had been characterized by SEM. In addition, Energy-dispersive X-ray spectroscopy (EDX) had been used to analyze the nanoparticles, which, were found in the membrane, pores. Figure 43(a) and (b), is showing a thin layer of nanoparticles, the EDX analysis for this layer indicated to these were silver nanoparticles.

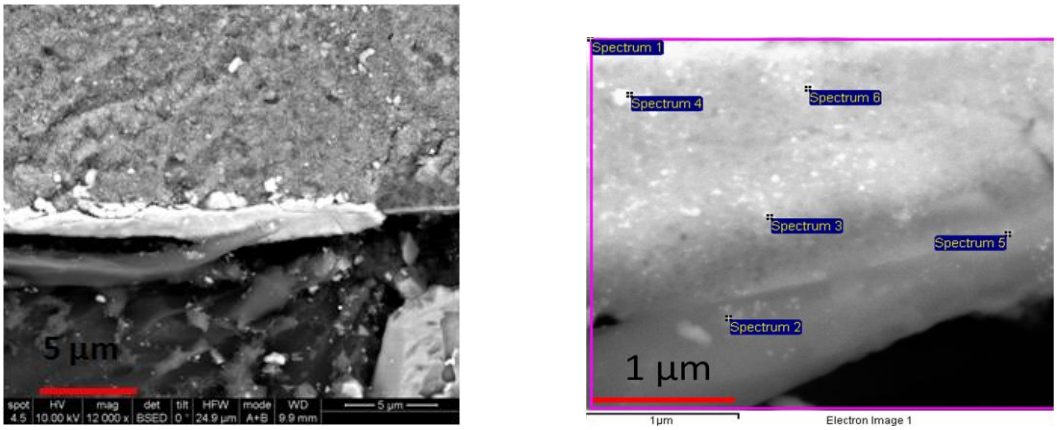

(a) (b)

Figure 43: SEM and EDX analysis for the 5 nm membrane after filtration.

Table 9 shows the results from EDX analysis for the nanoparticles which existing in the pores of the membrane and approving the existence of silver nanoparticles in all the places in addition to the titanium and aluminum.

Table 9: EDX analysis for the 5 nm membrane.

Spectrum	1	2	3	4	5	6	mean
Ag	1.70	1.92	2.64	1.83	1.56	0.88	1.75

Chapter five: Conclusion

The ultrasonic procedure of synthesis silica nanoparticles is non-reproducible method in terms of the particle mean diameter and the yield of the reaction. The conventional stirring method is a reproducible method taking into account : reasons:(1) controlling the addition of the tetraethyl orthosilicate as slow as possible, (2) Fixing the stirring rate from the beginning of the process and keep it constant, (3) Controlling the temperature of the stirring plat while the whole process at 30°C.

The fractionation process of the polydisperse and monodisperse silica solution using a cross flow filtration was successful using 60 nm membrane. Independently on the concentration of small nanoparticles is the feed, the membrane was able to fractionate the solution.

Additionally, the dead end filtration process was successful for purification and removal of the silver nanoparticles at low concentration 10 ppm (0.01 mg/ml) in 88 % rejection. The concentration of the silver in the filtrate solution was 2.1 ppm (0.0021mg/ml). The Uv-vis technique is not enough to evaluate the residue of the silver nanoparticles.

The cross flow filtration of polydisperse solutions of silver nanoparticles using 5 nm TiO_2/Al_2O_3 membrane was effective for fractionation the silver nanoparticles. The rejection of the membrane is inversely proportional to the concentration of the feed solution. As the silver nanoparticles of 0.5 mg/ml concentration lead to 95% rejection, while the 1 mg/ml concentration resulted to 48.2%, which is almost the half.

Bibliography

1. Kim, T., *Organic-solvent Resistant Ultrafiltration and Nanofiltration Membrane Modules for Separation and Purification of Nanoparticles*, in *Department of Chemistry*. November 3, 2011, Oregon State University: Oregon State University.
2. G.A. Mansoori , T.R.B., A. Ahmadpour, Z. and Eshaghi, *ENVIRONMENTAL APPLICATION OF NANOTECHNOLOGY* in *Annual Review of Nano Research* 2008.
3. Dhermendra K. Tiwari, J.B.a.P.S., *Application of Nanoparticles in Waste Water Treatment.* World Applied Sciences Journal 2008. **3(3)**: p. 417-433.
4. Bartlomiej Kowalczyk, I.L., Bartosz A. Grzybowski, *Nanoseparations: Strategies for size and/or shape-selective purification of nanoparticles.* Current Opinion in Colloid & Interface Science, 2011. **16**: p. 135–148.
5. Clarence Suh Yah, G.S.S.a.S.E.I., *Review: Nanoparticles toxicity and their routes of exposures.* Pakistan Journal of Pharmaceutical Sciences, April 2012. **25**(2): p. 477-491.
6. Trzaskus, K., *Nanoparticle filtration*, in *Netherlands Research School in Process Technology* U.o. Twente, Editor. 2011, www.ospt.eu.
7. Quan-Ling Xie, J.L., Xiao-Xiong Xu, Guo-Bin Han, Hai-Ping Xia, Xu-Min He, *Size separation of Fe2O3 nanoparticles via membrane processing.* Separation and Purification Technology 2009. **66**: p. 148–152.
8. Roberts, S.O.K.Z.-G.K.P., *Capillary electrophoretic separation of nanoparticles.* Analytical and Bioanalytical Chemistry, 2011. **399**: p. 2831–2842.
9. A.I. Lo´pez-Lorente, B.M.S., M. Valca´rcel, *Electrophoretic methods for the analysis of nanoparticles.* Trends in Analytical Chemistry, 2011. **30**(1).
10. M. Hanauer, S.P., I. Zins, A. Lotz, C. Sönnichsen, *Separation of Nanoparticles by Gel Electrophoresis According to Size and Shape.* Nano letters, 2007. **7**(9): p. 2881-2885.
11. Matthew Pelton, G.W.B., *Introduction to Metal-Nanoparticle Plasmonics*. GeneralTechnology & Engineering / Materials Science, ed. W.-S.W. Co-Publication. Vol. 5. 2013: John Wiley & Sons. 296.
12. Lee JS, S.S., Mirkin CA, *DNA-induced size-selective separation of mixtures of gold nanoparticles.* Journal of the American Chemical Society, 2006. **128**: p. 8899–903.
13. Orla M. Wilson, R.W.J.S., Joaquin C. Garcia-Martinez, and Richard M. Crooks, *Separation of Dendrimer-Encapsulated Au and Ag Nanoparticles by Selective Extraction.* Chemistry of Materials, 2004. **16**: p. 4202- 4204.

14. Sant, B.K.G.a.H.J., *Nanoparticle analysis using microscale field flow fractionation.* American Chemical Society, 2007. **6465**: p. 1-12.

15. Frank von der Kammer, S.L., Erik H. Larsen,Katrin Loeschner, Thilo Hofmann, *Separation and characterization of nanoparticles in complex food and environmental samples by field-flow fractionation.* Trends in Analytical Chemistry, 2011. **30**(3).

16. W. J . KOROS, Y.H.M.a.T.S., *Terminology for membranes and membrane processes (IUPAC Recommendation 1996).* Pure & Applied Chemistry, 1996. **68**(7): p. 1479-1489.

17. Hai-Wei Liang , L.W., Pei-Yang Chen , Hong-Tao Lin , Li-Feng Chen , Dian He , and Shu-Hong Yu, *Carbonaceous Nanofi ber Membranes for Selective Filtration and Separation of Nanoparticles.* Advanced Material 2010. **22**: p. 4691–4695.

18. Moataz M. Mekawy , A.Y., Sherif A. El-Safty , Tetsuji Itoh , Norio Teramae, *Mesoporous silica hybrid membranes for precise size-exclusive separation of silver nanoparticles.* Journal of Colloid and Interface Science 2011. **335**: p. 348–358

19. Scott F. Sweeney, G.H.W., and James E. Hutchison, *Rapid Purification and Size Separation of Gold Nanoparticles via Diafiltration.* JASC, 2006.

20. W. Stober, A.F.a.E.B., *Controlled Growth of Monodisperse Silica Spheres in the Micron Size Range.* Journal of Colloid and Interface Science, 1968. **26**: p. 62-69.

21. Ismail A.M. Ibrahim, A.A.F.Z., Mohamed A. Sharaf, *Preparation of spherical silica nanoparticles: Stober silica.* Journal of American Science, 2010. **6**(11).

22. Laura Gutierreza, L.G., , Silvia Irusta , Manuel Arruebo, Jesus Santamaria, *Comparative study of the synthesis of silica nanoparticles in micromixer–microreactor and batch reactor systems.* Chemical Engineering Journal, 2011. **171**: p. 674-683.

23. Yamamoto, T.Y., Hengbo. Wada, Yuji. Kitamura, Takayuki. Sakata, Takao. Mori, Hirotaro. . Yanagida, Shozo, *Morphology-Control in Microwave-Assisted Synthesis of Silver Particles in Aqueous Solutions.* Bulletin of the Chemical Society of Japan, 2004. **77**(4): p. 757-761

24. Angshuman Pal, S.S., Surekha Devi, *Microwave-assisted synthesis of silver nanoparticles using ethanol as a reducing agent.* Materials Chemistry and Physics 2009. **114**: p. 530-532.

25. Jenny N´ı Mhurch´u, G.F., *Dead-end filtration of yeast suspensions: Correlating specific resistance and flux data using artificial neural networks.* Journal of Membrane Science, 2006. **281** p. 325–333.

26. Baker, R.W., *MEMBRANE TECHNOLOGY AND APPLICATIONS*. 2004, England: John Wiley & Sons Ltd,. 538.

27. Munir, A., *Dead End Membrane Filtration*, in *Laboratory Feasibility Studies in Environmental Engineering*, S.A. Hashsham, Editor. 2006.

28. Instruments, M., *Dynamic Light Scattering:An Introduction in 30 Minutes* in *www.malvern.co.uk*, M.I. Ltd, Editor., Malvern Instruments Ltd: www.malvern.co.uk.

29. R. Das, S.S.N., D. Chakdar, G. Gope, R. Bhattacharjee, *Preparation of Silver Nanoparticles and Their Characterization.* AZo-OARS, 2009.

30. Asta ŠILEIKAITĖ1, I.P., Judita PUIŠO ,Algimantas JURAITIS, Asta GUOBIENĖ, *Analysis of Silver Nanoparticles Produced by Chemical Reduction of Silver Salt Solution.* MATERIALS SCIENCE, 2006. **12**(4): p. 287-291.

31. Geoffrey D. Moeser, K.A.R., William H. Green, and T. Alan Hatton, *High-gradient magnetic separation of coated magnetic nanoparticles.* AIChE, 2004. **50**(11): p. 2835-2848.

32. Szushen Ho, K.C., G. Daniel Lilly, Bongsup Shim and Nicholas A. Kotov, *Free flow electrophoresis for the separation of CdTe nanoparticles.* Journal of Materials Chemistry, 2009. **19**(10): p. 1390-1394.

33. Liu, F.-K., *Analysis and applications of nanoparticles in the separation sciences: A case of gold nanoparticles.* Journal of Chromatography A, 2009. **1216**: p. 9034-9047.

34. Williams, K.R., *What is field-flow fractionation?*, C.S.o. Mines, Editor.

Appendix

Appendix A: Methods of separation and fractionation of nanoparticles

1. Magnetic field

According to the nanoparticles size and/or their magnetic susceptibility the magnetic field can separate them with a magnetic force given by $FM=\mu 0\chi VpH\nabla H$; H is the external magnetic field, Vp is the particle volume and χ is the magnetic susceptibility . For iron oxide nanoparticle, theoretically the limit size for separation is ≈50 nm in the low magnetic field (< 100 T/m). Thermal diffusion and Brownian motion overcome the magnetic force affecting on the nanoparticle and it is not possible to get full fractionation in case of nanoparticle lower than 50 nm.

In the absence of the external magnetic field, the dipole-dipole interactions between particles' magnetic moments might be present. The formation of large nanoparticles aggregate could be happen because of these forces, these aggregation characterized by strong magnetic response. During high gradient magnetic separation (HGMS) of magnetic nanoparticles those aggregation were observed by Moeser et al. [31]. The formation of these aggregations also explains why it is possible to separate nanoparticles smaller than predicted by theory.

Capillary magnetic field flow fractionation (MFFF) is another system based on the magnetic field separation. According to this system, the nanoparticles can be separated not only by the different in the size but also by the different in the material composition. This technique depends on (i) the perpendicular magnetic forces to capillary flow and of magnitude proportional to the particles' magnetic susceptibility; and (ii) hydrodynamic forces and particle diffusion.[4]

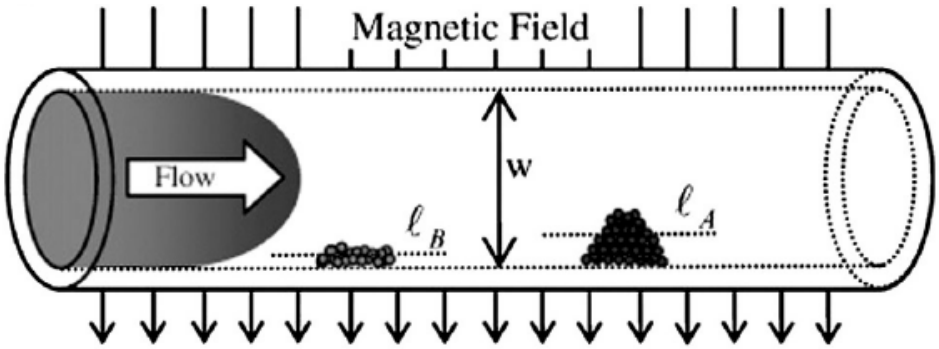

Figure a: Scheme illustrating the principle of MFFF for magnetic particles in a capillary channel subject to an applied magnetic field

2. Chromatography

In this system, the nanoparticles are separated based on the differences in the partition coefficients between mobile which containing a mixture to be separated and stationary phases for all components of the mixture. While high-performance liquid chromatography "HPLC" has been reported for many examples of the separation of the nanoparticles, the most popular chromatographic technique is size-exclusion chromatography (SEC) which used to fractionate nanoparticles. This system is separating nanoparticles not based on the interaction of these particles with the stationary phase but on the differences in the particles' hydrodynamic volumes.[4]

Particles in the range of a few ten- to a few hundred nanometers can be fractionated based on residence time differences in an SEC column packed with porous silica or other microporous particles. Figure b is showing scheme of size exclusion chromatography where the nanoparticles which are larger than the pore-size of the packing material are excluded and show no retention, while smaller nanoparticles are able to penetrate or permeate into the pore space of the packing material and are retained on the column in decreasing order of size.[1]

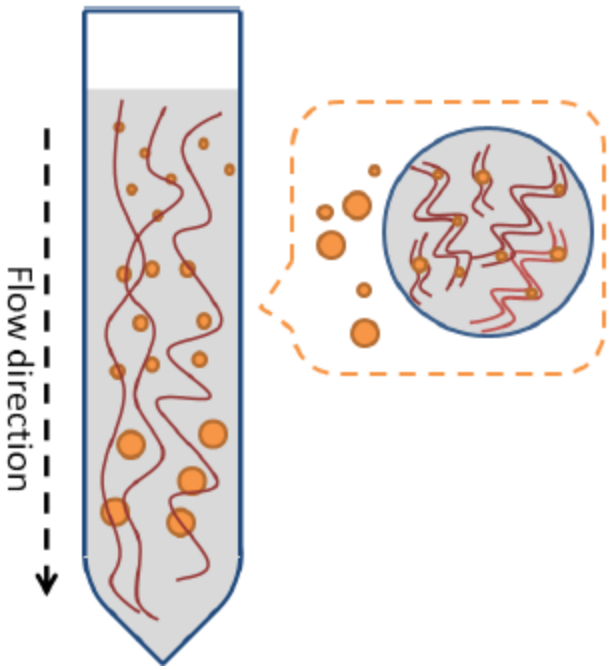

Figure b: SEC chromatography scheme

For successful resolution of a mixture by SEC, proper eluent and stationary phase (specifically, proper pore size of the stationary phase) have to be chosen, and irreversible adsorption of NPs onto the stationary phase (clogging its pores) should be avoided.[4]

3. Centrifugal and Density Gradient Centrifugal

In colloid science and in cellular and molecular biology, centrifugation could be considered one of the most important separation techniques, which is widely used. Density gradient centrifugal is one of the centrifugation techniques in which the density difference of the column of solution, which is containing the nanoparticle, is the base of separation. As a result, for the centrifugation the density is decreased from the bottom to the top of the tube.

In case of nanoparticles, density-gradient ultracentrifugation had been applied to the separation of different sized nanoparticles. The particle size differences affect the migration of

nanoparticles to the bottom of the test tube. While the high molecular weight nanoparticles are precipitated in the bottom, the small and light nanoparticles are remains in the supernatant.

However, the limitation of the sample amount, which can be separated in one tube, the time of the centrifugation and the high speeds, which needed for some cases, centrifugation is considered one of the less expensive and one of the most simple separation techniques.

In the following figure (figure c), the centrifugation tube is filled with solution with different gradient ratios and it shows the separation of different size nanoparticles using ultracentrifugation.[4],[1]

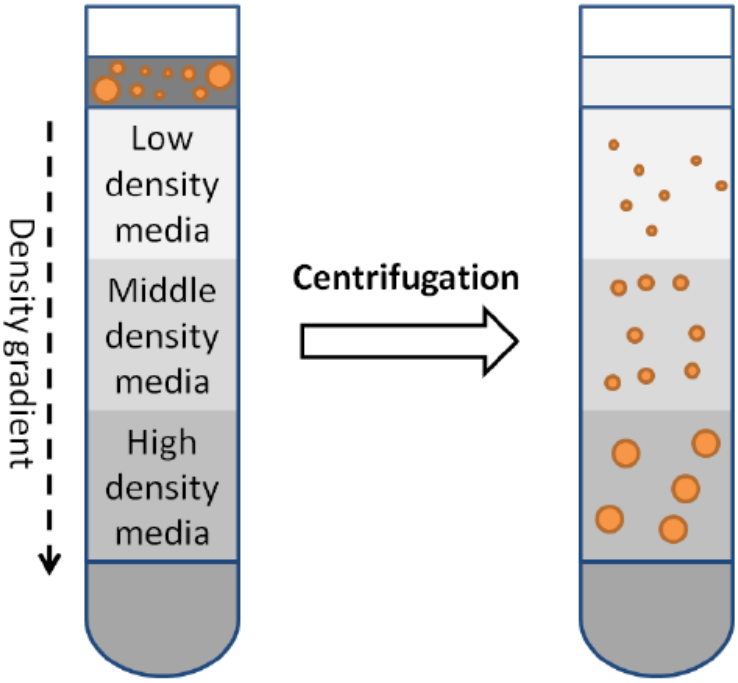

Figure c: Ultracentrifugation Scheme

4. Electrophoresis

Electrophoretic techniques can separate charged objects in a uniform electric field. These methods are used widely in biological and biochemical research, protein chemistry, and pharmacology. In an electric field the charged particles or molecules will migrate toward the opposite polarity electrode.[4] Gel electrophoresis (GE), free flow electrophoresis (FFE) and Capillary electrophoresis (CE) are the most used electrophoresis techniques.

In the field of nanoparticles separation and for the separation of biological macromolecules such as protein, DNA and RNA, gel electrophoresis (GE) is one of the most famous techniques. Although, it is highly time-consuming technique, many different successful fractionation had been reported though the retrieval of nanoparticles from sieving media. The detrimental effects on nanoparticles electrophoretic mobility of the viscous gel had limited the separation resolution [32]. Agarose gel electrophoresis had been used in the separation of metallic nanoparticles (gold and silver) having a charged polymer layer[10].

Figure d shows Optical micrographs of agarose gels supporting (GE) of nanoparticle mixtures. The dashed line at the bottom indicates the position of the gel wells. The four lanes contain, from left to right, silver nanoparticles, gold NRs (40×20 nm), gold rods and spheres mixed just before electrophoresis, and spherical gold NPs (15 nm) as indicated symbolically [10].

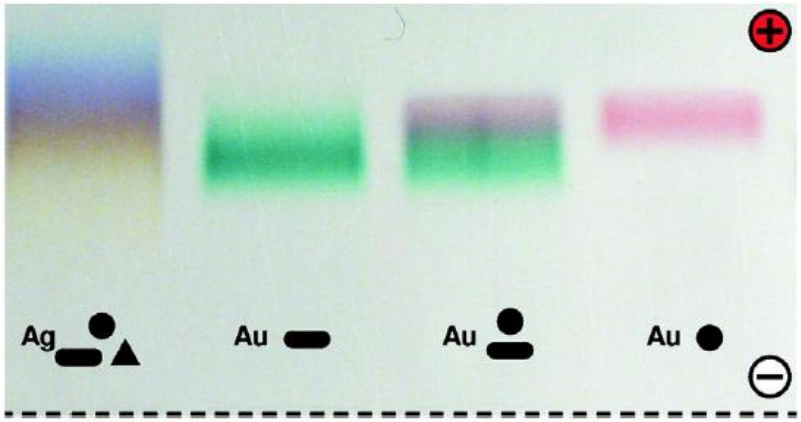

Figure d: Agarose gel electrophoresis [10]

On the other side, capillary electrophoresis (CE) is using the differences in the electrophoretic mobilities of particles in an electric field to separate them. The charge densities and radii of nanoparticles are suitable for successful capillary electrophoresis (CE) separation.[33]

Valca´rcel et al. had reviewed that different sized material such as inorganic oxides , metallic nanoparticles (silver and gold) and Carbon nanotubes had been separated by using capillary electrophoresis(CE) [9].

Comparing to other techniques, which had used to characterize nanoparticles such as electron microscopy, size-exclusion chromatography and a combination between high-performance liquid chromatography and the transmission electron microscope, capillary electrophoresis (CE) has reported as more useful, faster and with fewer surface effect. In addition to its advantages, capillary electrophoresis is a low consumption of sample and reagents [8], [9].

5. Size selective precipitation

The key to size selective precipitation is the different in size, shape and surface coverage .The chemical and physical properties and or stability are depending on the size of the particles.

Because of the strong dependent of those properties on the surface chemistry, size selective precipitation should be tailored to specific particle type/functionalization.

Mirkin et al. [12], discovered that there is a temperature which is called T_m . As a result to this discovery, at temperature above the so called Tm of smaller particles but below Tm of larger particles the separation of binary and ternary mixture of different sized (15, 30, 40, 50, 60 and 80 nm) into separated batches is possible with a purity could be higher than 90%. Figure e is showing TEM images showing the samples before and after fractionation for mixtures containing different sizes of NPs: (i) 15 and 60 nm; (ii) 30 and 60 nm; (iii) 40 and 80 nm.

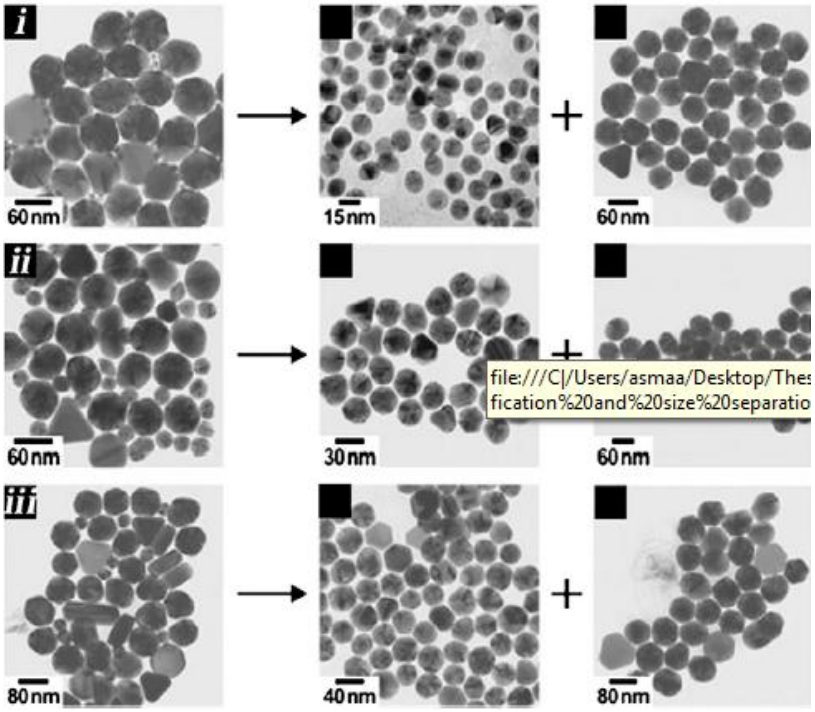

Figure e :TEM images showing the samples before and after fractionation for mixtures containing different sizes of NPs by size selective precipitation.[12]

6. L-L extraction

Liquid - liquid extraction (LLE) consists in transferring one (or more) solute(s) contained in a feed solution to another immiscible liquid (solvent). The solvent that is enriched in solute(s) is called extract. The feed solution that is depleted in solute(s) is called raffinate. Liquid–liquid extraction also known as solvent extraction and partitioning, is a method to separate compounds based on their relative solubilities in two different immiscible liquids, usually water and an organic solvent.

Wilson and co-workers [13] has reported the separation of Au and Ag dendrimer encapsulated nanoparticles from an aqueous mixture of the two using a selective extraction approach. In this work, an aqueous mixture of silver and gold dendrimer encapsulated nanoparticles has been separated by the addition of an *n*-alkanoic acid present in an organic solvent, which have a high affinity for Ag (but not Au).

The silver nanoparticles has selectively extracted through a strong ligand- nanoparticle interaction into the organic phase resulting in a solution of Ag monolayer-protected clusters. In addition, the remaining gold dendrimer encapsulated nanoparticles could be extracted after by the addition of an organic phase containing an *n*-alkanethiol. It is also possible to extract both metals simultaneously or selectively extract Au nanoparticles from a mixture of Ag and Au dendrimer encapsulated nanoparticles. Figure f is showing the separations schemes for both silver and gold dendrimer encapsulated nanoparticles.

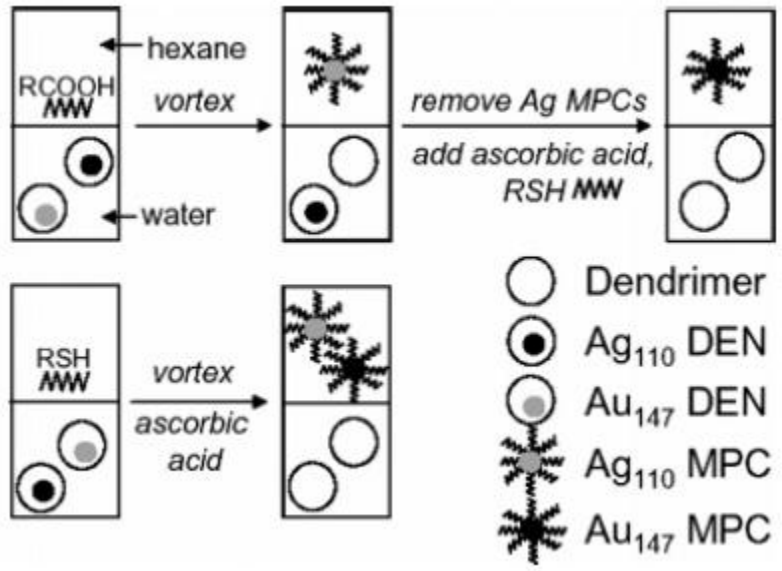

Figure f : Extraction separation schemes for both silver and gold dendrimer encapsulated nanoparticles [13].

7. Field-flow fraction (FFF)

Field-flow fractionation is a family of analytical and separation techniques that depend on the dual effect of the flow behavior and field distribution in a thin open channel. In addition, field-flow fractionation separations are carried out in a single phase compared to other techniques such as chromatography. The flow profile in field-flow fractionation channel can be described by a parabola with the highest flow velocity at the center of the channel and decreasing flow velocity

with increasing proximity to the channel walls. Field-flow fractionation channels typically consist of a thin spacer enclosed by two parallel plates, modified to impart the external field.

The sample mixture migrates toward one side of the channel by virtue of the channel flow, is lifted by diffusion and hydrodynamic forces, and sinks under the influence of the downward flow. Thus, the particle mixture distributes in the vertical direction; and particles are separated into zones of differing transport velocity[34] [1, 14].

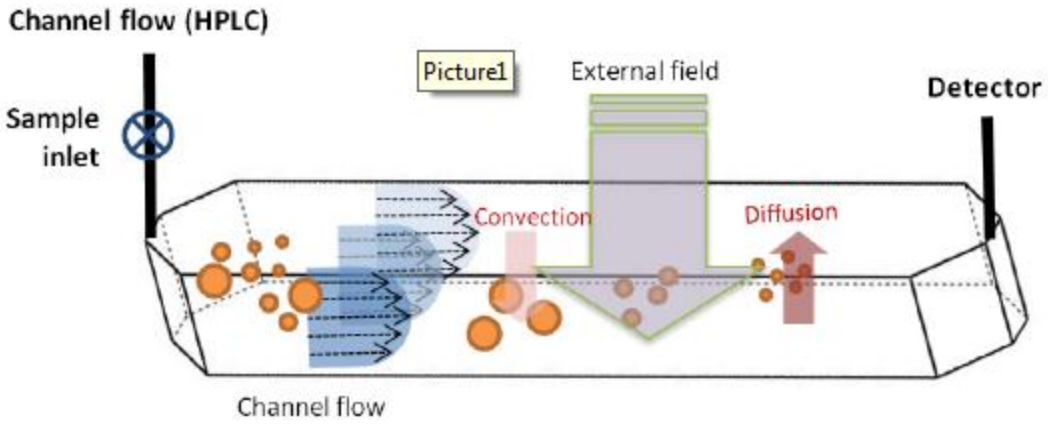

Figure g: Field flow fraction technique for particle size analysis[1].

Appendix B: Pictures of some equipment used for characterization

1. Dynamic light scattering

- Brookhaven 90 plus photo correlation spectroscope used for particle size analysis (DLS)

2. Transmission Electron Microscope

- FEI Technai T20 (LTEM) transmission electron microscope used for TEM characterization

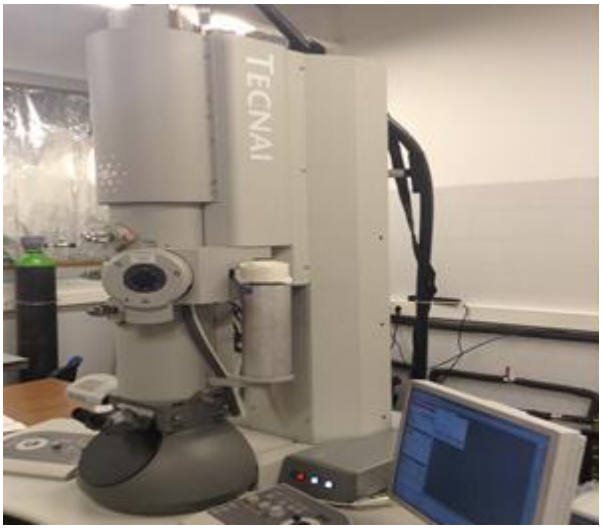

3. Ultraviolet–visible spectroscopy -UV-vis

Hellmanex JASCO V-670 spectrophotometer used for UV-vis characterization.

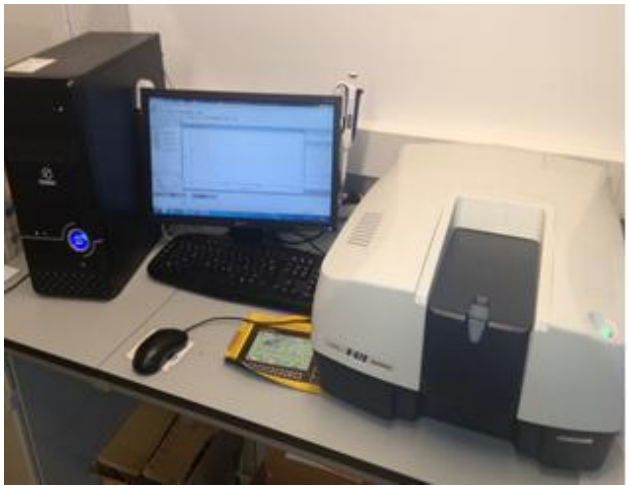

4. CEM discover single-mode microwave

CEM microwave system used to synthesize silver nanospheres.